ABSTRACT

ELECTROHYDRODYNAMICAL MANIPULATION OF PARTICLES BASED ON DIELECTROPHORESIS

by
Oleksii Vasylyschuk

The movement of matter in a non-uniform electric field, termed dielectrophoresis, is of interest to scientists of various branches: physics, chemistry, engineering, and life science. To chemists and physicists it is a science of many varied phenomena. To engineers it is a source of new and useful techniques for separating materials or improving materials' behavior. To ecologists it provides a major means of minimizing pollution. To life scientists it offers new ways to study and manipulate cells and their sub-particles, and to help unravel the nature of living systems.

The purpose of this thesis is to concentrate on some aspects of this powerful phenomenon in order to apply it to mechanical engineering problems. One of these particular engineering problems is development of a system for electrohydrodynamical manipulation of particles in fluids.

ELECTROHYDRODYNAMICAL MANIPULATION OF PARTICLES BASED ON DIELECTROPHORESIS

by
Oleksii Vasylyschuk

Blank Page

ELECTROHYDRODYNAMICAL MANIPULATION OF PARTICLES BASED ON DIELECTROPHORESIS

Oleksii Vasylyschuk

Dr. Nadine N. Aubry, Thesis Advisor   Date
F. Leslie and Milfred Jacobus Distinguished Professor of Mechanical Engineering,
Chair of Department of Mechanical Engineering, NJIT

Dr. Ernest S. Geskin   Date
Professor of Mechanical Engineering, NJIT

Dr. I. Joga Rao   Date
Assistant Professor of Mechanical Engineering, NJIT

BIOGRAPHICAL SKETCH

Author: Oleksii Vasylyschuk

Degree: Master of Science

Date: January 2003

Undergraduate and Graduate Education:

- Master of Science in Mechanical Engineering,
  New Jersey Institute of Technology, Newark, NJ, 2003

- Master of Science in Applied Physics and Mathematics,
  Moscow Institute of Physics and Technology, Moscow, Russia, 2000

- Bachelor of Science in Applied Physics and Mathematics,
  Moscow Institute of Physics and Technology, Moscow, Russia, 1998

Major: Mechanical Engineering

To my beloved family

ACKNOWLEDGMENT

TABLE OF CONTENTS

LIST OF TABLES

CHAPTER 1

INTRODUCTION

1.1 Application of Dielectrophoresis

The applications of dielectrophoresis are as follows

- Physics and Chemistry: general study of many varied phenomena

- Biomedicine: separation and manipulation of cells and their sub-particles

- Engineering: separation and manipulation of materials

General studies related to dielectrophoresis include the following topics: dielectric permittivity, positive and negative dielectrophoresis, dipole-dipole interaction, dielectric relaxation, double layer polarization, and other electrokinetic phenomena.

Many biomedicine and engineering applications are based on the separation and manipulation of particles, biological cells and their sub-particles. The separation of particles is based on the fact that when placed in a non-uniform AC electric field, polarized particles experience a variable translational force, depending on the applied field frequency. For particles whose polarizability is greater than the medium, the net movement takes place toward regions of highest field strength, whereas particles whose polarizability is less than that of the medium move to the regions of lowest field gradient. Because the particle's polarization is frequency dependent, the net force is also frequency dependent. Therefore, by judicious choice of suspending medium conductivity and applied frequency, even particles with very similar dielectric properties can be separated [Green and Morgan 1997].

1.2 Objective

The objective of this thesis is to present experimental results of the electrohydrodynamical manipulation of particles based on dielectrophoresis for two devices: macro-device and micro-device.

In order to define dielectric properties of the various materials used, a set of experiments was conducted. The efficiency of particles capturing was determined experimentally for both the macro- and micro-devices. These experiments allowed comparison of the efficiency of both devices and demonstrated that the miniaturization of the experimental device increases capturing efficiency of small particles.

CHAPTER 2

BACKGROUND INFORMATION

2.1 Dielectrophoresis in Liquids

Dielectrophoresis is the translational motion of neutral matter caused by polarization effects in a nonuniform electric field [Pohl 1978]. Electrophoresis is the motion caused by the response to free charge on a body in an electric field (uniform or nonuniform) [Shaw 1969]. Dielectrophoresis has a relatively simple physical origin. Any electric field, uniform or nonuniform, exerts a force upon a charged body. It is characteristic of nonuniform fields, however, that they exert a force upon neutral bodies.

It is helpful in considering the nature of the action of a nonuniform field upon neutral matter to compare the responses of charged and neutral bodies in both uniform and nonuniform fields. In a uniform electric field (Figure 2.1), a charged particle is pulled along the field lines towards the electrode carrying the charge opposite to that on the particle. In the same field, a neutral body will merely be polarized. The result may produce a torque in the neutral body, but not a net translational force, without which the body as a whole will not move toward either electrode. If the body is anisotropic in its polarizability, or if it is elongated, a torque can arise. The resultant dipole tends to align itself in the field. If the particle is isotropic and spherically symmetric, no torque will arise.
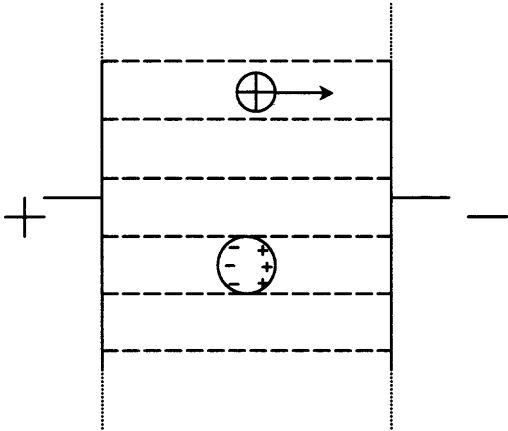
Figure 2.1 Behavior of neutral and charged bodies in a uniform electric field.
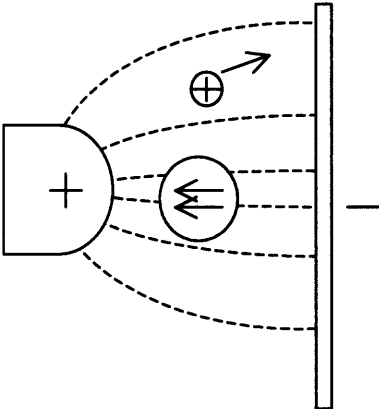
Figure 2.2 Behavior of neutral and charged bodies in a nonuniform electric field.

Different behaviors of the charged and uncharged objects in a non-uniform field are shown in Figure 2.2. The charged one behaves much as before, being pulled along the field lines. It is still attracted toward the electrode of opposite polarity. The neutral particle will in this case find a translational force upon it. This occurs because under the influence of the nonuniform field it acquires a polarization that has the effect of putting a negative charge upon the side nearer the positive electrode, and a positive charge on the side nearer the negative electrode. Since the particle is neutral, the two charges on the body are in fact equal. However, the fields operating on the two regions are unequal. This gives rise to a net force. The usual result of such polarization of a neutral body in a nonuniform field is to bring about a force impelling the neutral body toward the region of stronger field.

Notice that in the case of a nonuniform electric field acting upon neutral particles, which electrode is positive and which one is negative has no relevance to the force acting on neutral particles. For this reason, the applied electric field can be that due to an alternating potential (see Figure 2.3). This contrast between the behavior of charged and neutral bodies in a rapidly reversing or alternating field is a very noticeable one. The charged body, if under only the influence of electrophoresis, tends to merely vibrate about its original position. The neutral object, if under the influence only of dielectrophoresis, will, in contrast, tend to move steadily into the region of higher or lower field intensity.

(a)   (b)
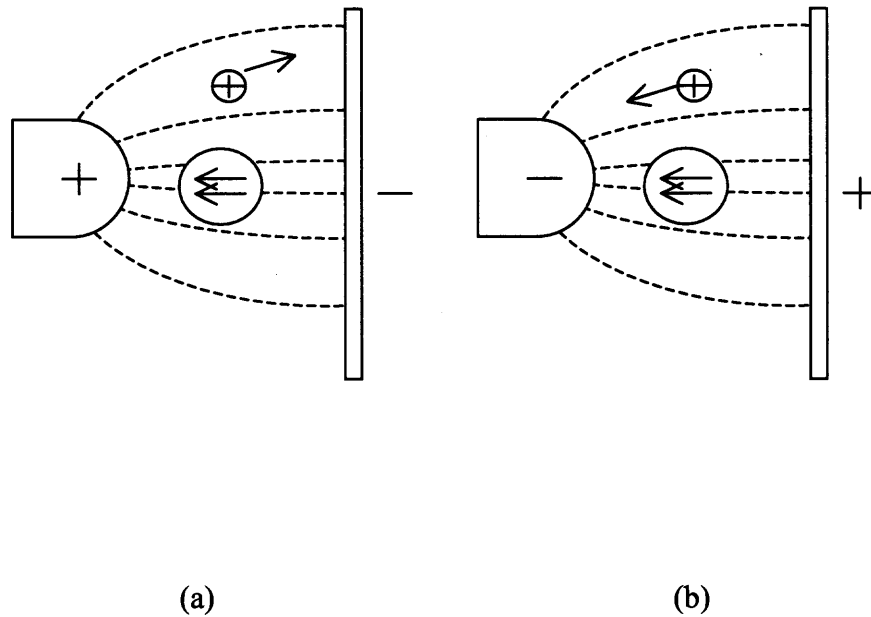
Figure 2.3 Comparison of behaviors of neutral and charged bodies in an alternating nonuniform electric field.

(a)   A positively charged body moves towards the negative electrode. A neutral body is polarized, and then attracted towards the region where the electric field is strongest or weakest. Since the two charged regions in the neutral body are equal in amount of charge, a net force towards the region of more intense field results.

(b)   A positively charged body moves towards the negative electrode. Again, the neutral body is polarized, but does not move in reverse direction although the electric field is reversed. It still moves towards the region of highest or lowest field intensity.

Before proceeding with a more detailed study of dielectrophoresis, it will be helpful to compare dielectrophoresis and electrophoresis carefully.

Dielectrophoresis arises from the polarization of matter, and from the subsequently differing forces at the two ends of the dipole, because of the differing electric fields in the two regions of a nonuniform electric field. This tends to force the polarized body into regions of differing field strength. Electrophoresis arises from the direct action of an electric field upon a charged particle.

Some of the contrasts between dielectrophoresis and electrophoresis are given below [Pohl 1978].

1) Dielectrophoresis produces the motion of bodies suspended in a fluid medium. The direction of that motion is independent of the sign of the field. Accordingly, either AC or DC fields can be used. Electrophoresis produces a motion of suspended particles in which the direction of the resultant path depends upon both the sign of the charge on the particle and the sign of the field direction. Reversal of the field reverses the direction of travel.

In practice, care must be taken in the application since both electro- and dielectrophoresis can be present simultaneously. On occasion, the motion of charged particles can be towards a sharp electrode if an AC field of high strength is present. This occurs because of space charge effects and the appearance of partial rectification or selective charge injection.

2) Dielectrophoresis gives rise to an effect, which is proportional to the particle volume while electrophoresis is proportional to the particle charge. Dielectrophoresis is therefore more easily observed on coarse particles. It is observable at the molecular level only under special conditions. Electrophoresis is observable with particles of any size such as atomic ions, molecular ions, charged colloidal particles, or charged macroscopic bodies.

3) Dielectrophoresis usually requires quite divergent fields for strong effects. Electrophoresis operates in both uniform and divergent fields.

4) Dielectrophoresis requires relatively high field strengths. In media of low dielectric constant (say 2-7) the electric field strength is usually of the order of 10^4 Vm^{-1}. In media of higher dielectric constant (e.g. water, 80) lower fields may be used successfully (500 Vm^{-1}).

With previously charged particles (e.g. ions, charged sols), electrophoresis requires relatively low fields. Strong fields can evoke space charging in the fluid (gas or

liquid) dielectric, with subsequent deposition of charges upon previously neutral particles, and a resultant electrophoretic force.

Dielectrophoresis usually requires a substantial difference in the relative permittivities of the particle and surrounding medium. Electrophoresis can be significant even when the free charge per unit weight of the particle is quite small. Unlike dielectrophoresis, it does not depend upon the particle volume *per se* (and hence upon the total polarization available), but rather upon the free charge on the particle.

Dielectrophoresis deposits weight of coarse sol proportional to the applied voltage during equal times of deposition. It is a relatively gentle effect, most readily observed on large particles in gases or liquids of low viscosity. The fields should normally be high, but controlled in order to avoid undue heating or space-charge effects. Dielectrophoresis can often be masked by competing side effects such as convection, flow turbulence, or electrophoresis.

2.2 Positive and Negative Dielectrophoresis

When the permittivity (dielectric constant) of the particles exceeds that of the suspending medium, the collection, or positive dielectrophoresis, occurs [Pohl 1978]. When the permittivity of the particles is less than that of the suspending medium, no collection in the regions of higher field intensity occurs. Instead, negative dielectrophoresis occurs, i.e., movement of the particles into regions of lower field intensity.

Therefore, it is possible to separate particles according to their dielectric properties alone. Particles of the same size could be successfully separated. Since it is virtually impossible to separate small particles of similar size but with different biological

properties, nanoscale dielectrophoresis may find new applications in separating a range of structures such as chromosomes, viruses, DNA and macromolecules [Green and Morgan 1997].

For example, non-viable cells often have membranes that are degraded to the extent that ions can readily diffuse across them, unlike membranes for viable cells whose resistance to non-specific ion diffusion is very large. This allows for their mixture to be separated.

2.3 Dielectric Permittivity

According to Zaky and Hawley [1970], the total dielectric permittivity can be shown as

$$\varepsilon = \varepsilon_\infty + \frac{\varepsilon_s - \varepsilon_\infty}{1 + j\omega\tau} \tag{2.1}$$

where ω is the frequency of the alternating electric field. Here, τ refers to the relaxation time of the electric medium and determines the rate at which the polarization builds up; it is independent of the frequency but depends upon the temperature. The other variables are ε_s or static value of the relative permittivity and ε_∞, the value of the relative permittivity at high frequency. The relative permittivity of the material is the ratio of the absolute dielectric permittivity of the material to the dielectric permittivity of free space $\varepsilon_0 = 8.854 \ast 10^{-12}$ C/Vm.

Separating the real and imaginary parts, the dielectric permittivity can be written as

$$\varepsilon = \varepsilon' - j\varepsilon'' \tag{2.2}$$

where

$$\varepsilon' = \varepsilon_\infty + \frac{\varepsilon_s - \varepsilon_\infty}{1 + \omega^2 \tau^2} \qquad (2.3)$$

is the real part of permittivity, and

$$\varepsilon'' = \frac{(\varepsilon_s - \varepsilon_\infty)\omega\tau}{1 + \omega^2 \tau^2} \qquad (2.4)$$

is the imaginary part of permittivity.

These equations are known as the Debye relaxation equations [Tallan, 1974]. At zero frequency, ε' is equal to the static value of the relative permittivity and ε'' is zero. At sufficiently high frequencies such that $\omega\tau \gg 1$, $\varepsilon' = \varepsilon_\infty$ and ε'' is negligibly small. The maximal value of ε'' is reached when $\omega\tau = 1$. Thus, by determining the frequency at which ε'' is maximal, the relaxation time τ may be found.

Table 2.1 gives the relative permittivity of a number of dielectric materials; the values given are for static or low frequency (<1000 c/s) fields [Zaky and Hawley 1970], [Hippel 1995], [Solymar and Walsh 1998].

The relative permittivity of a material is a directly measurable quantity, which expresses on a microscopic scale the overall result of the interaction between an externally applied field and the atoms or molecules of the material considered. This interaction is referred to as polarization.

Table 2.1 The Relative Permittivity of Some Solid Dielectrics at 25^0C.

Material	ε_r	Source
Amber	2.7	Zaky and Hawley, 1970
Borosilicate glass	4	Zaky and Hawley, 1970
Corning glass 0010	6.68	Zaky and Hawley, 1970
Corning glass 0014	6.78	Zaky and Hawley, 1970
Pyrex glass	4~5	Zaky and Hawley, 1970
Quartz (fused)	3.8	Zaky and Hawley, 1970
Diamond	5.5	Zaky and Hawley, 1970
Porcellain	5.5	Zaky and Hawley, 1970
Marble	10~15	Zaky and Hawley, 1970
Mica	6~11	Zaky and Hawley, 1970
Steatite	6	Zaky and Hawley, 1970
Polyethylene	2.25	Solymar and Walsh, 1998
Polyvinylchloride	6	Solymar and Walsh, 1998
Epoxy resin	3.6~11	Zaky and Hawley, 1970
Rubber	3~4	Zaky and Hawley, 1970
Neoprene	7	Zaky and Hawley, 1970
Beeswax	2.65	Zaky and Hawley, 1970
Paraffin wax	2.3	Zaky and Hawley, 1970
Barium Titanate	1200	Zaky and Hawley, 1970
Al_2O_3	8.6	Hippel, 1995; Solymar, 1998
TiO_2	70	Hippel, 1995; Solymar, 1998
$ZrSiO_4$	12.5	Hippel, 1995; Solymar, 1998
SiC	10	Hippel, 1995; Solymar, 1998

2.4 Dielectrophoretic Force

The instantaneous dielectrophoretic force on a particle, $F(\omega)$, as a function of the frequency of the electric field applied, is given by [Green and Morgan 1997]

$$F(\omega) = \text{Re}\{(m(\omega)*\nabla)E\} \qquad (2.5)$$

where m is the field induced dipole moment of the particle, E the electric field and Re indicates the real part.

For a spherical particle of radius a, the induced dipole moment is given by the following well-known equation

$$m = 4\pi\varepsilon_0 f(\varepsilon_p, \varepsilon_m)a^3 E \qquad (2.6)$$

where

$$f(\varepsilon_p, \varepsilon_m) = \varepsilon_m \frac{\varepsilon_p - \varepsilon_m}{\varepsilon_p + 2\varepsilon_m} \qquad (2.7)$$

ε_m and ε_p being the complex permittivities of the medium and the particle; $\varepsilon_0 = 8.854*10^{-12}$ C/Vm is the permittivity of free space.

Therefore, the force on the sphere becomes

$$F = 2\pi a^3 \varepsilon_0 \, \text{Re}\left\{\varepsilon_m^* \frac{\varepsilon_p - \varepsilon_m}{\varepsilon_p + 2\varepsilon_m}\right\}\nabla|E|^2 \qquad (2.8)$$

where * denotes the complex conjugate.

The real part of the Equation (2.7) is

$$\beta(\varepsilon_p, \varepsilon_m) = \frac{(\varepsilon_p' + 2\varepsilon_m')(\varepsilon_m'(\varepsilon_p' - \varepsilon_m') + \varepsilon_m''(\varepsilon_p'' - \varepsilon_m'')) + (\varepsilon_p'' + 2\varepsilon_m'')(\varepsilon_m'\varepsilon_p'' - \varepsilon_m''\varepsilon_p')}{(\varepsilon_p' + 2\varepsilon_m')^2 + (\varepsilon_p'' + 2\varepsilon_m'')^2} \qquad (2.9)$$

where ε' and ε'' are the real and imaginary parts of permittivity.

Metallic particles, which have an almost infinitely high polarizability, show a dielectrophoretic force upon them greatly affected by the much lesser conductivity of the aqueous medium.

The motion of the particles inside the experimental device can be described by the following equation of the force balance

$$F_{inertia} + F_{hydrodinamic} + F_{dielectrophoresis} = 0 \tag{2.10}$$

$$m\frac{dU_p}{dt} = 6\pi\mu a(U_f - U_p) + 2\pi a^3\varepsilon_0 \, \mathrm{Re}\{f\}E.\nabla E \tag{2.11}$$

where U_p is the velocity of the particles and U_f is the velocity of the fluid.

The inertia force can be neglected because it is much smaller in magnitude than the other forces. The gravitational force is not included in the expression for the force balance, because the density of the particles is very close to the density of the fluid, and therefore, this force is negligible. It follows that

$$0 = 6\pi\mu a(U_f - U_p) + 2\pi a^3\varepsilon_0 \, \mathrm{Re}\{f\}E.\nabla E \tag{2.12}$$

The motion of each particle can be calculated by integrating Equation (2.12).

The Equation (2.12) can be non-dimensionalized by introducing the characteristic length L, velocity U_f, voltage V and time scale L/U_f to it. The characteristic length L is the distance between two electrodes, the velocity U_f is the average velocity of the flow and V is the applied voltage. Therefore, Equation (2.12) can now be introduced in dimensionless form

$$0 = 6\pi\mu a(U_f - U_p)\frac{L}{U_f} + 2\pi a^3\varepsilon_0 \, \mathrm{Re}\{f\}E.\nabla E\left(\frac{V}{L}\right)^2\frac{1}{U_f L} \tag{2.13}$$

or, equivalently,

$$(U_p - U_f) + \frac{1}{Mn}(E.\nabla E) = 0 \tag{2.14}$$

with
$$Mn = \frac{3\mu}{\text{Re}\{f\}\varepsilon_0 a^2} \frac{U_f L^3}{V^2} \tag{2.15}$$

where Mn is Mason number, which is the ratio of the hydrodynamic force to the dielectrophoretic force.

2.5 Double Layer Polarization

There are six interesting effects, all due to the existence of a diffuse and mobile ion double layer at phase interfaces [Bottcher 1973-78]. These are grouped under the general name of electrokinetic phenomena. The first four involve the slippage of the outer mobile portion of the double layer past the fixed solid portion below. These phenomena are: electrophoresis, streaming potential, electroosmosis, and the Dorn effect. The fifth and sixth phenomena involve the distortion of the outer portion of the double layer relative to the fixed inner layer. They are often referred to as electric-field-induced and mechanically-induced double layer polarization. A simplified sketch of the double layer is shown in Figure 2.4 [Smyth 1955].

The experimental response due to electric double layer polarization in a nonuniform field [Pohl 1978], dielectrophoresis (Figure 2.5), depends upon the square of the applied field intensity. This is because the polarization producing the dipole depends upon the field strength to the first power, but the response of the dipole to the field gradient is also proportional to the field strength. The combination of the two components produces square field dependence.
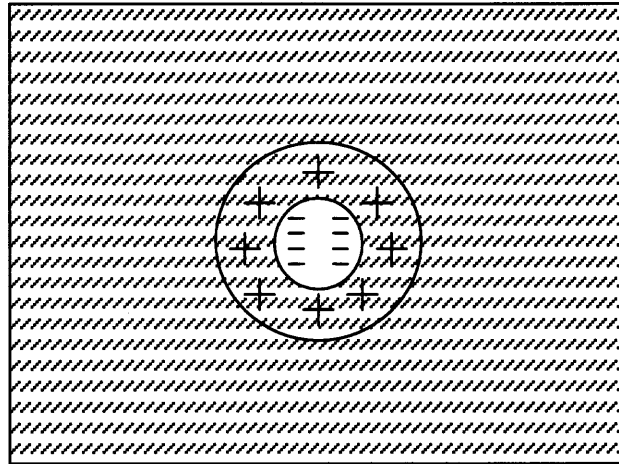
Figure 2.4 Double layer polarization before applying a field.
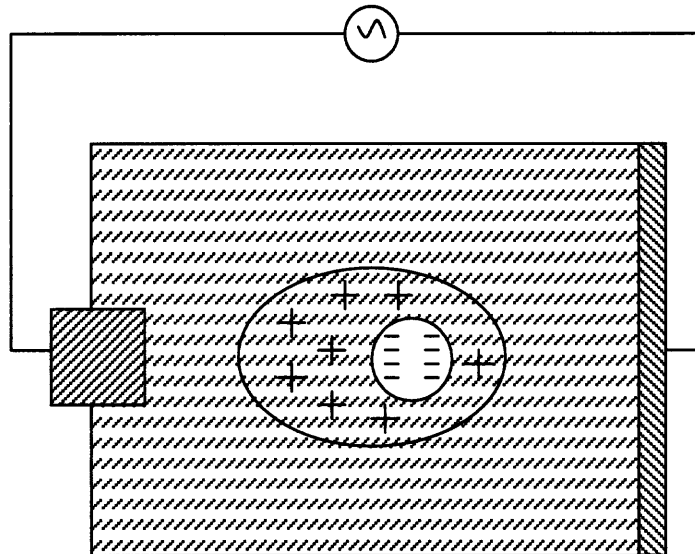

Figure 2.5 Double layer polarization after applying an alternating electric field.

In a broad sense, it may be noted that the region of contact between two different materials, generally of differing work functions or chemical potentials, will give rise to an interfacial potential and thereby a dipolar surface layer. In the event that one or both of the materials are easily dissociated or are of high dielectric constant, dissociation of the surface dipolar layer into ionic species can be understood to occur. The origin of the primary charge at the surface of a colloidal particle can be more particularly attributed to specific interactions such as absorption, adsorption, covalent bonding, van der Waal's forces, or a highly localized Columbic force.

An infinitesimally thin layer can be considered, but the possibility of ion exchange with the surrounding electrolyte has to be neglected. It is well known that the counterions on the surface of a charged particle are, or can be, strongly bound by electrostatic attraction. Provided that there are defects in the surface lattice, the bound counterions can move much more easily along the surface than away from it. It was assumed by Schwarz [Pohl 1978] that the counterions near the charged surface are bounded to it so firmly that an external field cannot detach them, but that they can be displaced along the surface by the tangential component of the field. This, according to the bound-layer model, will result in an effective polarization of the bound-ion atmosphere and the induction of a large electric dipole moment for the particle.

2.6 Mutual Dielectrophoresis

The bunching effect is the clumping or bunching of a group of neutral particles caused by the action of the applied field. It is particularly evident when particles of high dielectric constant suspended in a medium of lower dielectric constant are subjected to an external

field and undergo dielectrophoresis. Particles undergoing dielectrophoresis often exhibit a mutual attraction. Suspended particles are often observed to clump or bunch together, even in the presence of an apparently uniform external field. This is referred to as mutual dielectrophoresis [Pohl 1978], and arises in the following way. Particles, which have a polarizability different from that of the surrounding medium, distort the field. Each particle then experiences a nonuniform field created by the other particles.

The dielectrophoretic interaction of uncharged dielectric particles in an electric field is responsible for the strong chain formation exploited in electrorheological fluids and electrofusion of cells. This same electrostatic force is an important mechanism for particle cohesion in electrostatic precipitators and electrofluidized beds. The electrostatic adhesion of particles to a conducting or dielectric surface closely related may be thought of as the interaction of a particle and its electrostatic image [Washizu and Jones, 1996].

2.7 Dielectrophoresis of DNA Molecules

Deoxyribonucleic Acid (DNA) is the genetic material of all cellular organisms and most viruses. DNA carries the information needed to direct *protein synthesis* and *replication*. Protein synthesis is the production of the proteins needed by the cell or virus for its activities and development. Replication is the process by which DNA copies itself for each descendent cell or virus, passing on the information needed for protein synthesis. In most cellular organisms, DNA is organized on chromosomes located in the nucleus of the cell.

A DNA molecule consists of base pairs (bp), the estimated size of which is 0.333 nanometers [Washizu and Kurosawa 1990]. The length of a DNA molecule is 72 - 23,130

base pairs (bp). A DNA molecule has the charge of one electron per nucleotide, consisting of half of the base pair charge. In media with pH factors different from pH factor of the water, DNA has different charges; so one refers to the charge of a DNA molecule inside some particular medium.

Fingerprinting of DNA, also called DNA typing, makes it possible to compare samples of DNA from various sources in a manner that is analogous to the comparison of fingerprints. In this procedure, scientists use restriction enzymes to cleave a sample of DNA into an assortment of fragments. Solutions containing these fragments are placed at the surface of a gel to which an electric current is applied. The electric current causes the DNA fragments to move through the gel. Gel consists of small channels in which DNA fragments are subjected to frictional force. Frictional force is bigger on larger DNA fragments, therefore larger DNA fragments move through the gel slower than smaller fragments. Because smaller fragments move more quickly than larger ones, this process, called gel electrophoresis, separates the fragments according to their size. The fragments are then marked with probes and exposed on X-ray film, where they form the DNA fingerprint—a pattern of characteristic black bars that is unique for each type of DNA. The approximate time of the experiment is 6 hours.

In order to improve separation and analysis of DNA molecules, a comparison of the dielectrophoretic and electrophoretic forces on DNA has to be performed.

Using the fact that the permittivity of DNA is infinite, it can be shown that the real part of $f(\varepsilon_p, \varepsilon_m)$ is equal to 1. Therefore, the expression for the dielectrophoretic force becomes much simpler

$$F(\omega) = \varepsilon_m a^3 (E.\nabla)E \qquad (2.16)$$

The value of the expression (E.∇)E was taken as 10^{17} V^2/m^3.

The expression for the electrophoretic force is

$$F = QE = 2eNE \tag{2.17}$$

where e is the charge of an electron, N is the number of base pairs in a DNA molecule and E is the electric field strength.

The value of E during electrophoresis of DNA is usually 150-200 V/cm = 15,000-20,000 V/m. The comparison of the dielectrophoretic and electrophoretic forces on DNA, calculated from the Equations (2.16-2.17), is shown in Figure 2.6.
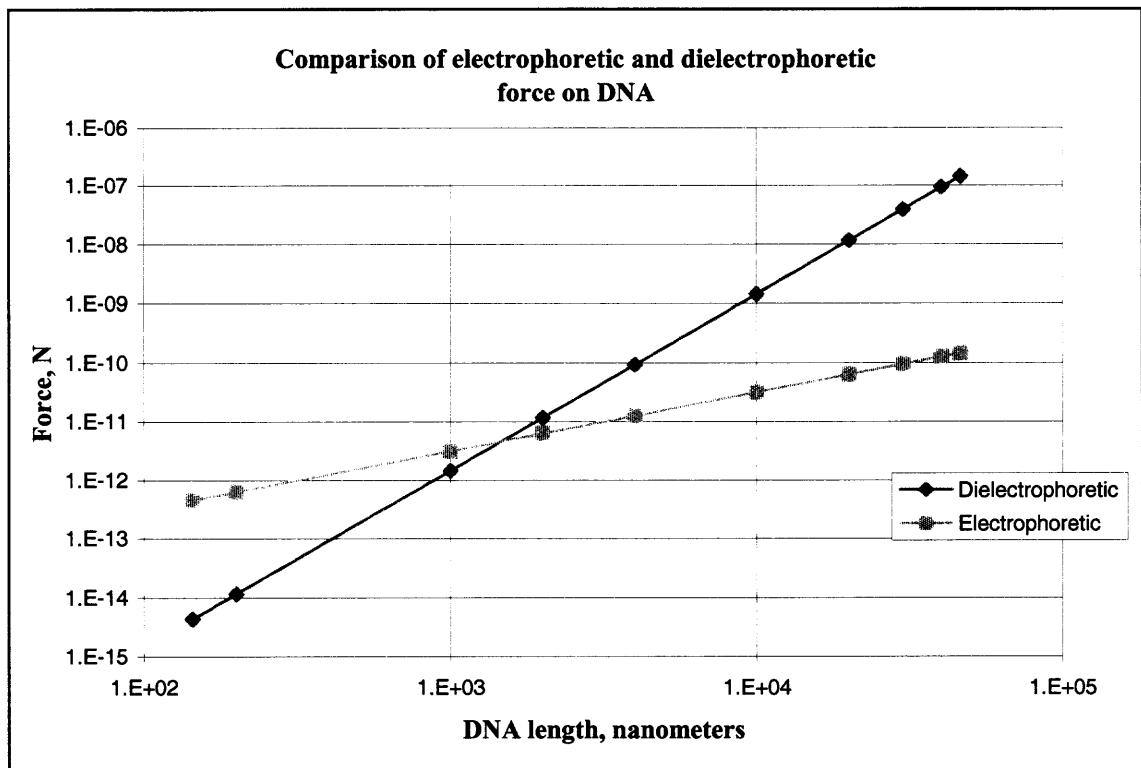

Figure 2.6 Comparison of dielectrophoretic and electrophoretic force on DNA.

The above comparison of the dielectrophoretic and electrophoretic forces on DNA shows that the growth of the dielectrophoretic force with DNA size is much larger than the growth of the electrophoretic force. This means that dielectrophoretic separation and analysis of DNA can be done more precisely than in the case of electrophoresis [Washizu 1995]. In addition, as the DNA molecule is stretched along the field lines, it becomes more susceptible to the dielectrophoretic effect [Washizu 1994; Suzuki 1998]. This stretching of DNA can potentially be used for the manipulation and molecular surgery of DNA [Yamamoto, 2000].

Dielectrophoresis can also be used for the handling of biological cells using a fluid integrated circuit [Washizu, Nanba, and Masuda, 1990]; this phenomenon could be used for the dielectrophoretic detection of molecular bindings [Kawabata and Washizu 2001] and the measurement of bacterial motor characteristics [Washizu 1993].

CHAPTER 3

EXPERIMENTAL SET UP

3.1 Materials and Devices

Diesel fuel oil was used for all experiments on the manipulation of particles. The density of diesel fuel oil is $\rho_{oil}=8.2*10^5$ (g/m^3), its dynamic viscosity $\mu_{oil}=2*10^{-2}$ (N*s/m^2), and its kinematic viscosity is $v_{oil}=2.4*10^{-8}$ (m^2/s).

In order to simulate the contamination of oil, FM-1 and FM-2 Ceramic Microspheres from PQ Corporation were used. FM-1 Ceramic Microspheres contain mullite, glass and up to 5% crystalline silica. FM-2 Ceramic Microspheres contain mullite, and glass exclusively. Both of them have a bulk density $4*10^2$ kg/m^3 and a density in suspension $8.1*10^2$ kg/m^3. FM-1 and FM-2 powders were sieved to have particle sizes ranging from 2 to 75 micrometers.

Initially, measurements of dielectric constants were conducted for both the particles and the oil using the AIS Alpha High Resolution Dielectric Analyzer in the NJIT W.M. Keck laboratory. The AIS High Resolution Dielectric Analyzer is a device for measuring with high precision the impedance or complex dielectric function of materials of frequencies in the range 3µHz-10 MHz.

Model 8000A of HIAC/ROYCO Particle Counter was used to quantify the capturing efficiency of both macro- and micro-devices. This is a digital, 8-channel particle counter that provides processing, control, and flexibility for use in batch or in on-line particulate contamination analysis. The Model 8000A Counter includes a 24-key keypad for input, a 40-column 16-line LCD display and a 40-character line graphics

printer for output to the operator. The counter and operator input/output are controlled independently by integral microprocessors that communicate with each other when required over an interconnecting bus structure.

The optical microscope Nikon Eclipse ME600 was used to observe particulate flows and measure particle velocities in the experimental devices. This system not only delivers images with brilliant sharpness, but also allows users to configure it to match their specific needs with the attachment of various accessories.

The KODAK Motion Corder Analyzer SR-500 with the camera connected to the optical microscope Nikon Eclipse ME600 was used to measure particle velocities and record images of the flow in digital format. The Motion Corder SR-500 offers speed up to 500 frames per second and utilizes an electronic shutter to minimize motion blur.

The peristaltic pump MITYFLEX with Masterflex L/S Easy-Load pump head was used to generate the fluid flow in the system. The MITYFLEX variable speed drives are powered by a DC gearmotor. A specially designed electronic speed control system provides smooth acceleration control over the entire flow range. The three-position on/off switch allows the user to maintain the speed setting when the unit is turned of or reversed. The experimental devices flow rates were set to 125 mL/min for the macro-device and to 2.03 mL/min for the micro-device. These flow rates corresponded to the same flow velocity in both devices.

The Wavetek Model FG2A 2 MHz function generator was used to create an AC electric signal with particular voltage and frequency. This function generator is a wide-range instrument capable of producing signals in the 0.2 Hz to 2.0 MHz range. In order to amplify this signal to the desired level, the Trek Model 10/40 high voltage amplifier was

used. The Model 10/40 is a DC-stable, high-voltage power amplifier designed to provide precise control of output voltages in the range of 0 - ± 10 kV DC or peak AC with an output current range of 0 - ±40 mA DC or peak AC. It is configured as a noninverting amplifier with a fixed gain of 1000 V/V. Fluke 8840A multimeter was used to control voltage during experiments. Therefore, for the macro-device, an AC sine wave electric signal of 2000V and 600 Hz was used to create electric field strength of 2 MV/m. For the micro-device to create the same electric field strength, an AC electric signal of 500 V and 600 Hz was used.

The macro-device consisted of a horizontal parallel set of channels that were $7.94*10^{-2}$ m long, $1.59*10^{-3}$ m wide and $9.53*10^{-3}$ m high. Thirteen parallel interdigitated electrodes formed a set of twelve channels. The top view of the cell is shown in Figure 3.1. The configuration was such that electrodes connected to the AC electric field source alternate with grounded electrodes.

The micro-device consisted of a horizontal parallel set of micro-channels that were $7.94*10^{-2}$ m long, $2.5*10^{-4}$ m wide and $9.53*10^{-3}$ m high. Three parallel interdigitated microelectrodes formed a set of two micro-channels. The top view of the micro-cell is shown in Figure 3.2. The central electrode is grounded while the two peripheral electrodes are connected to the AC electric field source.
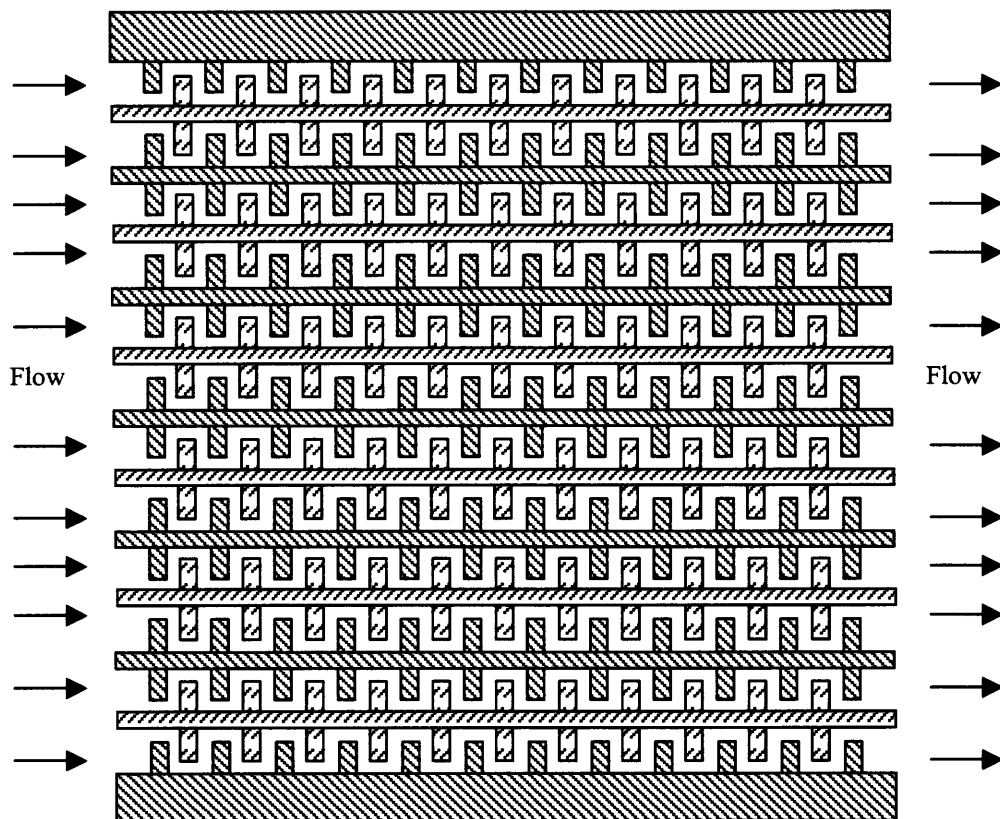
Figure 3.1 Schematic top view of macro-cell.
- electrodes connected to the source of AC electric field.
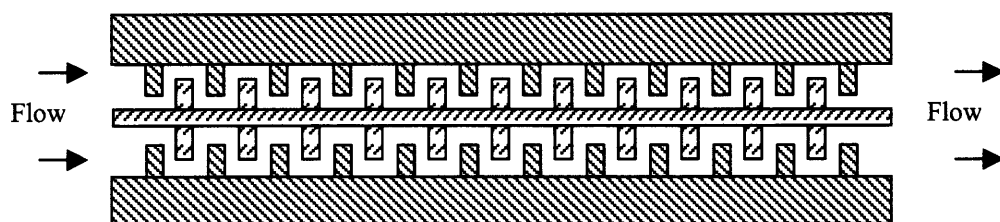- electrodes connected to the ground.

Figure 3.2 Schematic top view of micro-cell.
- electrodes connected to the source of AC electric field.
- electrodes connected to the ground.

3.2 Experimental Approach

The main purpose of the experiments is to capture and manipulate different types of particles suspended in diesel fuel oil using dielectrophoresis.

The approach, used in this work, consists in (i) using materials with known properties, (ii) making exclusion of the influence of the gravitational, (iii) using positive dielectrophoresis, and (iv) utilizing pearl-chain formation.

In this work pure diesel oil and well-defined particles were used. The term "well-defined" means that all of the physical properties of the particles are known (including dielectric properties, size distribution, density and shape). Furthermore, in order to avoid the influence of the gravitational field, particles with almost the same density as the density of diesel oil were selected.

The next step is to use positive dielectrophoresis instead of negative dielectrophoresis. One of the reasons why positive dielectrophoresis was chosen in this study is that natural contaminations in oils are subjected to positive dielectrophoresis. The other reason is that areas of a lower gradient of electric field intensity are usually larger than the areas of higher gradient of electric field intensity. This is why particles collected near electrodes under the action of negative dielectrophoresis are less immobilized than those drawn to the electrode edges by positive dielectrophoresis [Wang and others 1993; Markx and Pethig 1995].

The last step is to use a pearl-chain formation, which is caused by mutual dielectrophoresis between particles and can be useful for increasing the capturing efficiency of experimental devices. This phenomenon increases the effective area of electrodes by capturing particles on already captured ones.

The experimental procedures for the macro- and micro-devices are similar and can be described as follows.

The suspension of particles in diesel fuel oil was obtained by adding 0.1 g of FM-1 or FM-2 particles to 500 mL of oil. The solution was stirred for five minutes and a sample of 150 mL was extracted. The particle counter was used to measure the concentration of particles in this suspension and that data was recorded as initial concentration. The experimental device was assembled and oriented on the bench so that the flow was directed upwards. It was connected to the oil container through tubing hoses, and one of the hoses was connected to the pump in order to create a flow through the device. After creating sufficient flow through the device, the AC electric field was turned on. At the end of the experiment, a sample of 150 mL of oil was extracted from the container, whose particle concentration was measured and recorded as the final concentration. By subtracting the final concentration from the initial concentration of particles, the concentration of captured particles and therefore the efficiency of the device were deduced.

CHAPTER 4

RESULTS AND DISCUSSION

4.1 Dielectric Constants of Materials

The experimental values of relative dielectric permittivity of different materials are shown in Figures 4.1-4.3, where Eps' is the real part of permittivity, Eps" is the imaginary part and Eps (total) is the total dielectric permittivity of the material.
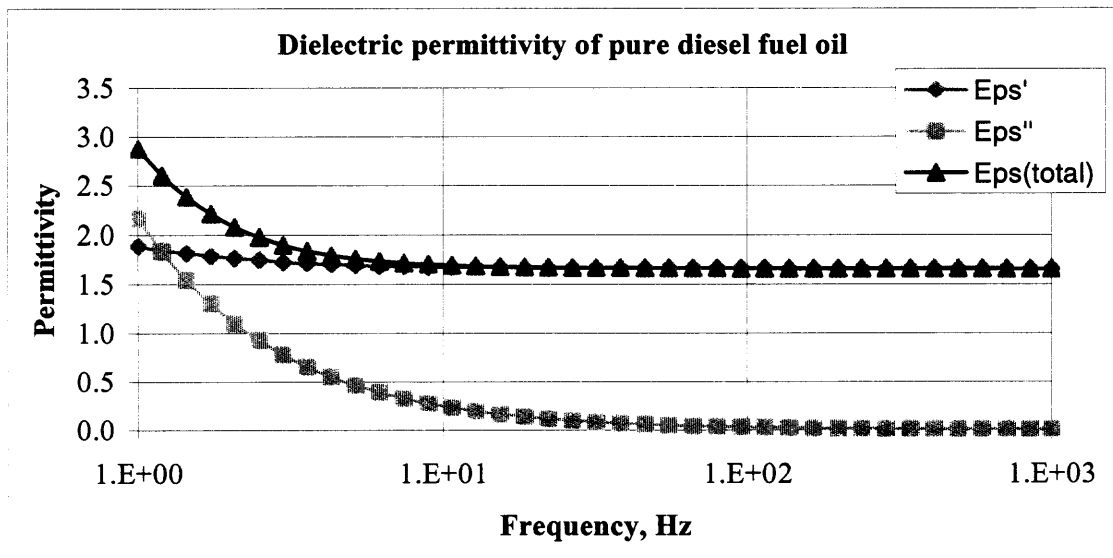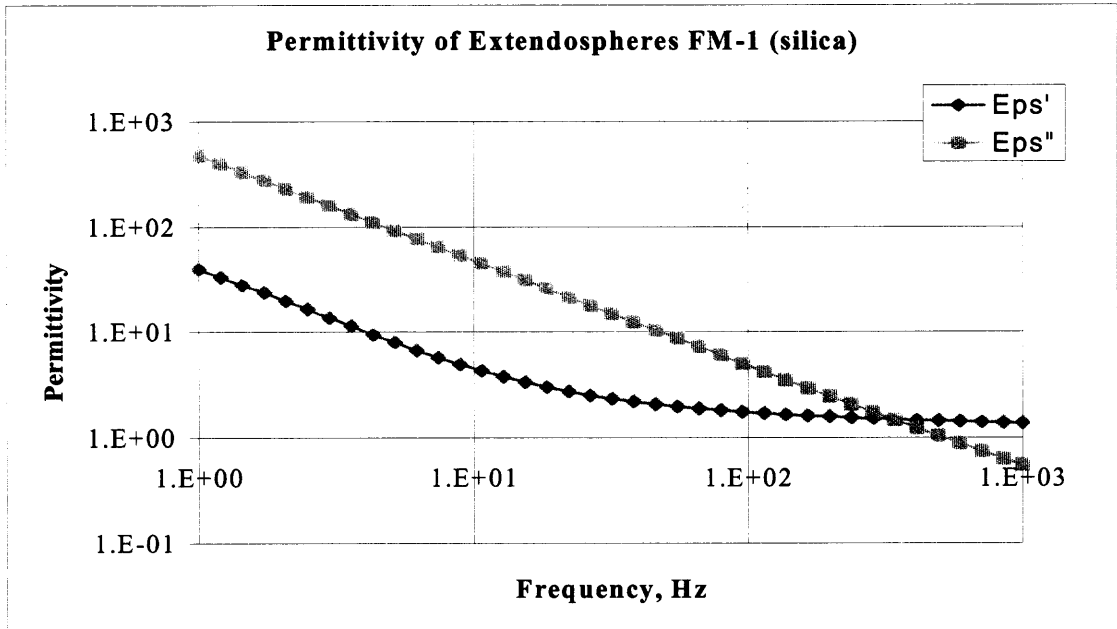
Figure 4.1 Dielectric permittivity of pure diesel fuel oil.
Eps' is the real part of permittivity; Eps" is the imaginary part of permittivity; Eps (total) is the total dielectric permittivity of material.
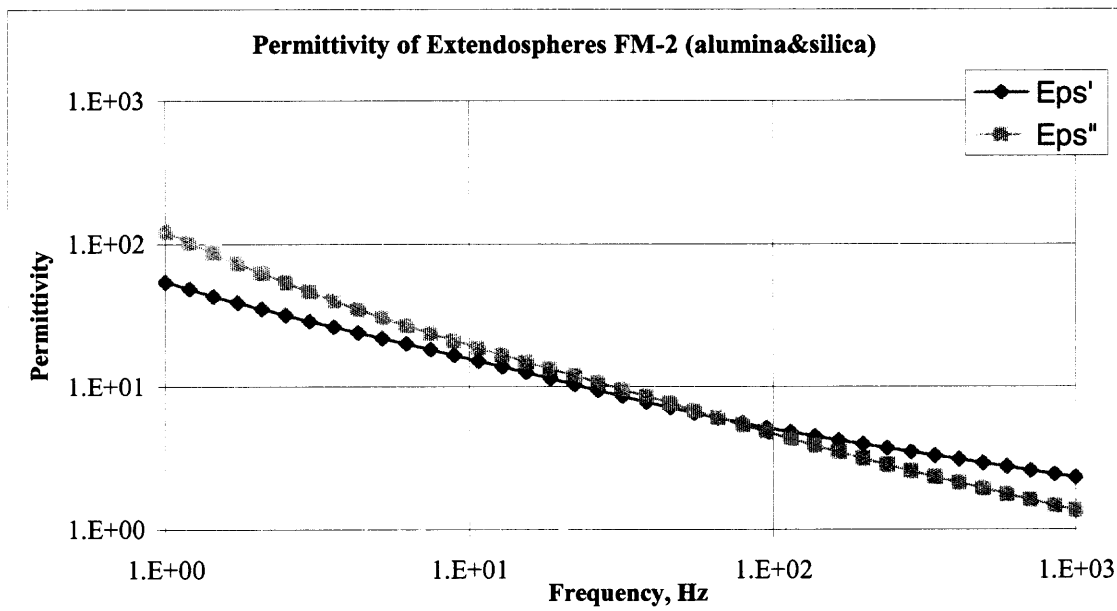
The values of the dielectric permittivity for pure diesel fuel oil shown in Figure 4.1 are typical for oils (the value of the total dielectric permittivity Eps (total) for oils usually lies in the range 1.6 - 3).

Figure 4.2 Dielectric permittivity of FM-1 particles.
Eps' is the real part of permittivity; Eps" is the imaginary part of permittivity; Eps (total) is the total dielectric permittivity of material.

Figure 4.3 Dielectric permittivity of FM-2 particles.
Eps' is the real part of permittivity; Eps" is the imaginary part of permittivity; Eps (total) is the total dielectric permittivity of material.

The values of the real part of the dielectric permittivity for FM-1 and FM-2 particles shown in Figures 4.2 – 4.3 are very close to each other, while the imaginary parts are more distinguishable.

The real part of $f(\varepsilon_p, \varepsilon_m)$, was calculated for both combinations (diesel fuel oil - FM-1 particles) and (diesel fuel oil - FM-2 particles) from Equation (2.9). The sign of the real part of $f(\varepsilon_p, \varepsilon_m)$ predicts which type of dielectrophoresis (positive or negative) occurs in the experimental system: when this sign is positive – dielectrophoresis in the system is positive; when the sign is negative – dielectrophoresis in the system is negative.
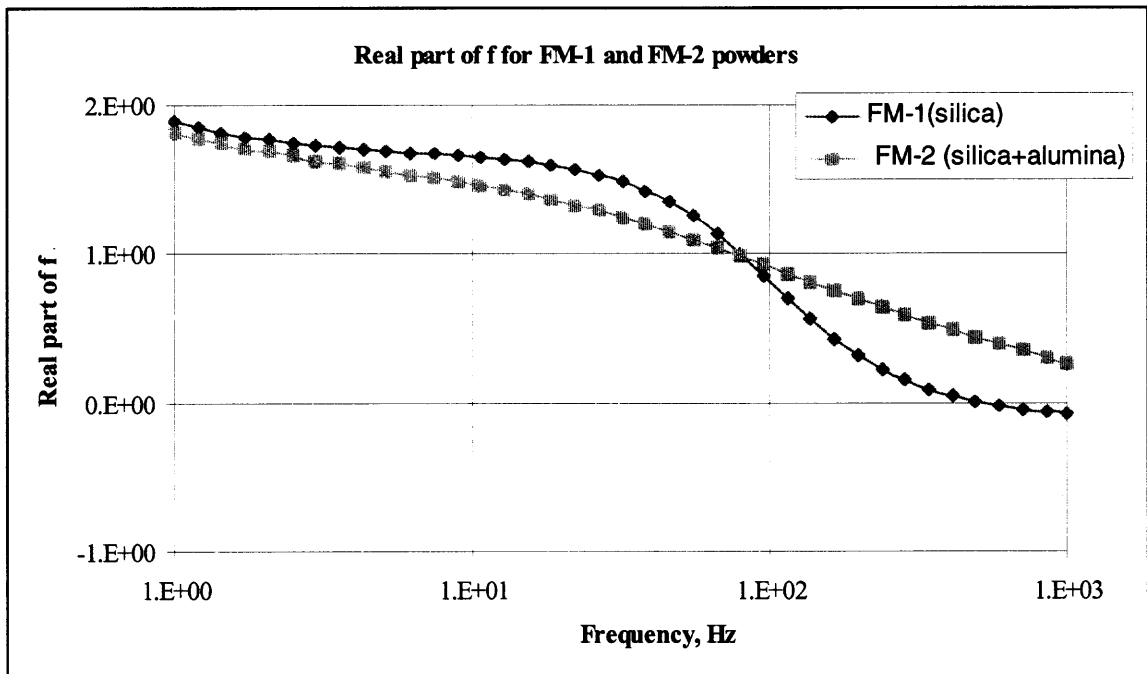
Figure 4.4 Comparison of the real part of $f(\varepsilon_p, \varepsilon_m)$ for FM-1 and FM-2 particles.

Conducted experiments show that positive dielectrophoresis can be observed for the combinations (diesel fuel oil - FM-1 particles) and (diesel fuel oil - FM-2 particles). The occurrence of positive or negative dielectrophoresis in the system depends on the frequency of the AC electric field. The 600 Hz frequency of the AC electric field was selected for these experiments.

4.2 Particles Velocity Measurement

It is known (see Chapter 3) that the density of diesel fuel oil is $\rho_{oil}=8.2*10^5$ g/m^3, while its dynamic viscosity is $\mu_{oil}=2*10^{-2}$ N*s/m^2, and kinematical viscosity is $\nu_{oil}=2.4*10^{-5}$ m^2/s. The flow Reynolds number was calculated using the formula

$$Re = Vd/\nu \qquad (4.1)$$

where V is the velocity of the oil, and d is the width of the channel.

The width of the macro- and micro-channels are $d_1=1.58*10^{-3}$ m and $d_2=2.5*10^{-4}$ m, respectively. The optimal flow rate in the macro-channel was found experimentally to be $Q_1=125$mL/min$=2.08*10^{-6}$ m^3/s. The cross sectional area of the macro-channels is $S_1=1.8*10^{-4}$ m^2, while it is $S_2=4.8*10^{-6}$ m^2 for the micro-channels. The average velocity of the suspension at the entrance of the macro-channel was calculated from the flow rate and the cross sectional area, using $V_{av1}=Q_1/S_1= 1.16*10^{-2}$ m/s. Therefore, the maximal velocity of the oil at the entrance of the macro-channel was found to be equal to $V_1=1.5*V_{av1}=1.74*10^{-2}$ m/s. Using this velocity, the Reynolds number in the macro-channel was calculated: $Re_1=V_1d_1/\nu_{oil}=1.15$. The optimal flow rate in the micro-channel was found experimentally to be $Q_2=2.03$ mL/min $= 3.4*10^{-8}$ m^3/s. Therefore, using the formula (4.3) with the maximal fluid velocity at the entrance of the micro-channel equal

to $V_2=1.06*10^{-2}$ m/s, the Reynolds number in the micro-channel was calculated: $Re_2=V_2 d_2//v_{oil}=0.11$.

The total volume of the oil in the system for the macro-device was equal to $V_1=325$ mL and the total volume of the oil in the system for the micro-device was equal to $V_2=175$ mL. Therefore, the time required for one pass of the total volume of the oil through the system was calculated as follows

$$T = \frac{V}{Q} \tag{4.7}$$

Using the above formula, the time of one pass $T_1=2.6$ min for the experiments with the macro-device and $T_2=86$ min=1.44 hours for the experiments with the micro-device was calculated. For the experiments with the macro-device, the time periods of 30 min and 3 hours were used, which corresponds to twelve and sixty-nine passes, respectively. For the experiments with the micro-device, time period of 3 hours was used, which corresponds to two passes.

4.3 Comparison of Results for Macro- and Micro-Device

Experimental results for the capturing efficiency of the macro- and micro-devices with FM-1 and FM-2 particles are given in this section. In order to estimate the time the macro-device takes to reach maximal capturing efficiency, experiments with time lengths of 30 minutes and 3 hours were conducted. Only one time length was selected for the micro-device because the flow rate there was very small and for 3 hours of experiment, only two passes of total volume could be achieved.

The initial concentration of FM-1 particles in diesel fuel oil for both experiments using the macro-device is shown in Figure 4.5. The cumulative number of FM-1 particles

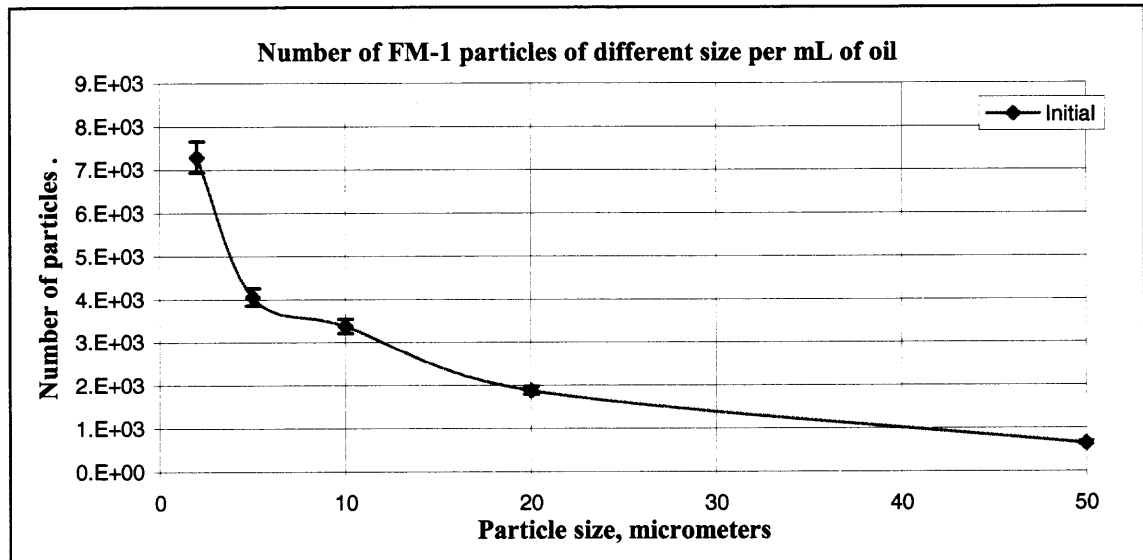of all sizes per mL of diesel fuel oil at the beginning of 30 minutes and 3 hours experiments was about 17000.

Figure 4.5 Initial number of FM-1 particles of different sizes per mL of diesel fuel oil.

The capturing efficiency of the macro-device with FM-1 particles over a run time of 30 minutes (corresponding to twelve passes of the total volume of the oil in the system) is displayed in Figure 4.6. This figure shows that the capturing process was not maximal during that time duration. Next, the average capturing efficiency of the macro-device with FM-1 particles over a run time of 30 minutes is shown in Figure 4.7. This average capturing efficiency was calculated from the data shown in Figure 4.6. The error bars in Figures 4.6-4.7 correspond to an error of 5%, including the error of the particle counter. The value of the capturing efficiency was the largest for FM-1 particles with sizes in the range of 10-20 micrometers. The capturing efficiency for FM-1 particles with sizes ranging from 50 to 75 micrometers was found to be lower than that for the particles of the smaller size because of the low concentration of these particles.
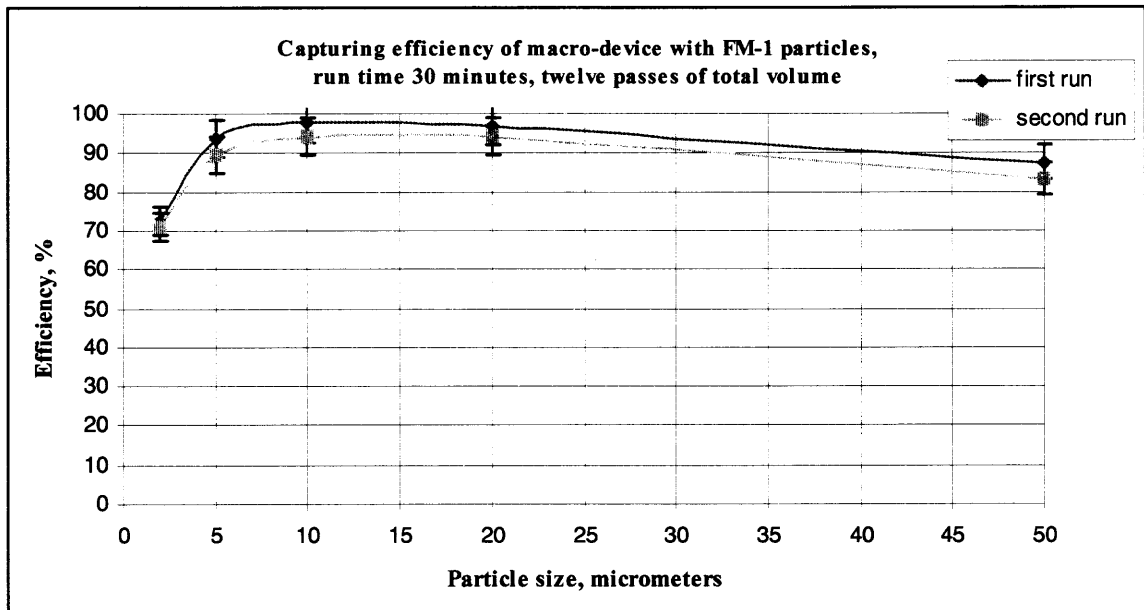
Figure 4.6 Capturing efficiency of the macro-device with FM-1 particles over a run time of 30 minutes, corresponding to twelve passes of the total volume.
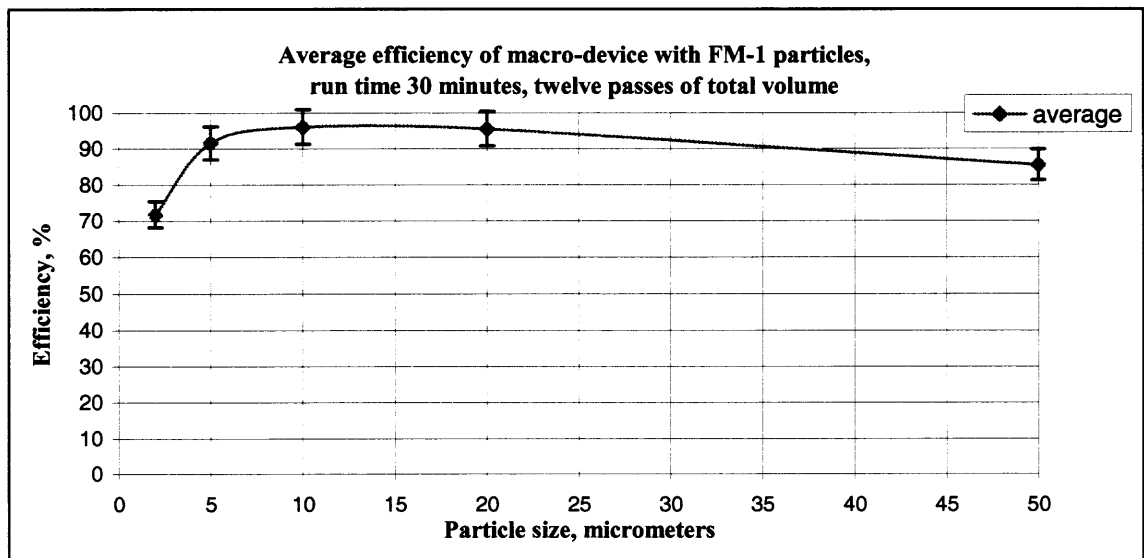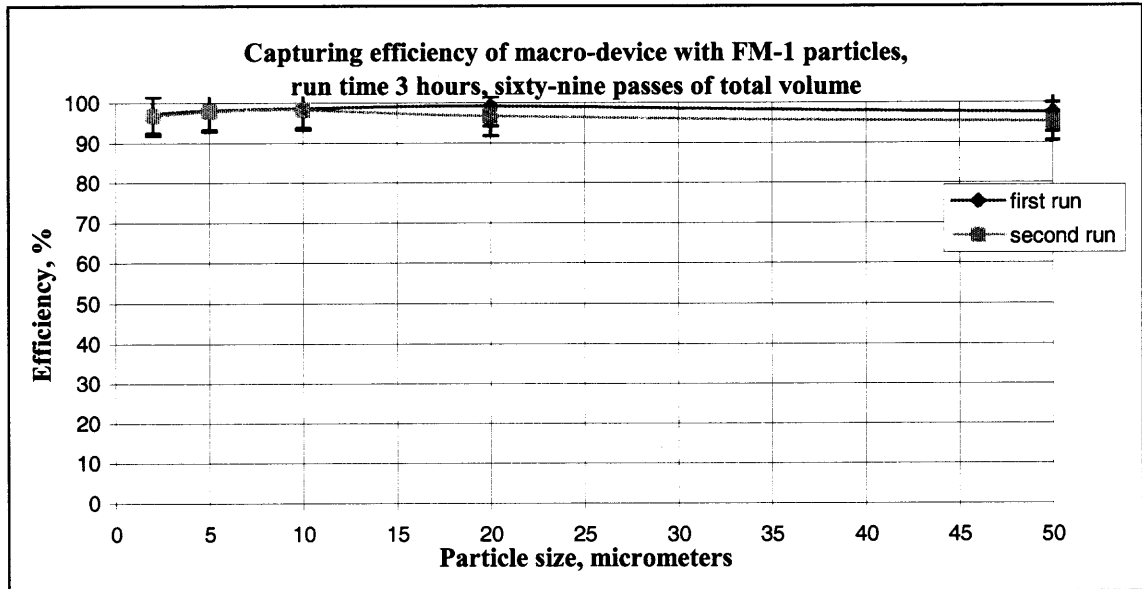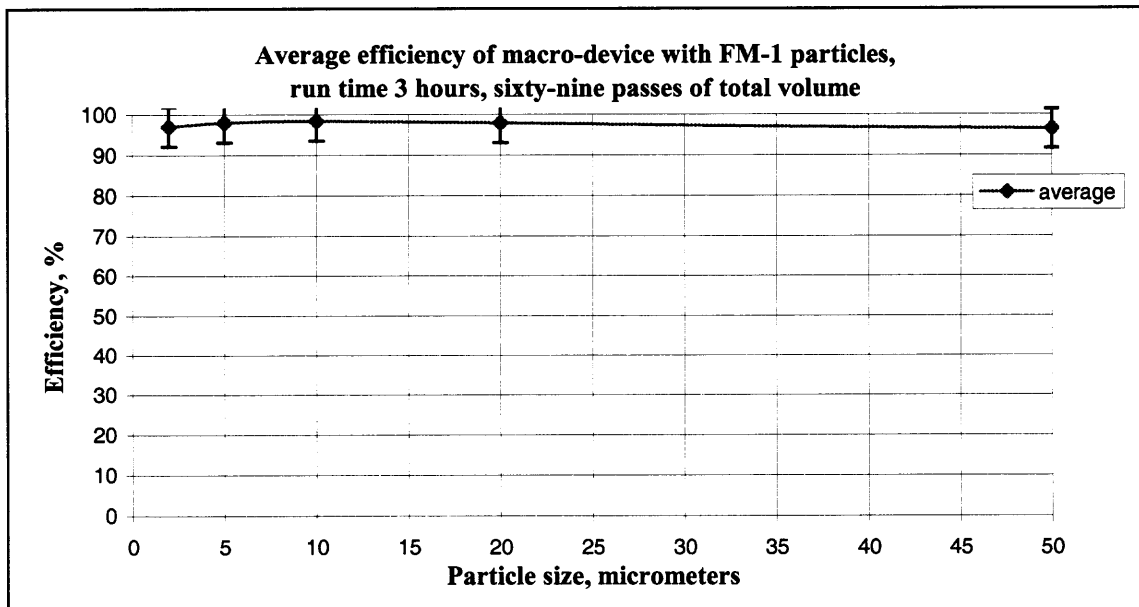

Figure 4.7 Average capturing efficiency of the macro-device with FM-1 particles over a run time of 30 minutes, corresponding to twelve passes of the total volume.

The capturing efficiency of the macro-device with FM-1 particles over a run time of 3 hours, corresponding to sixty-nine passes of the total volume of the oil in the system, is shown in Figure 4.8.

Figure 4.8 Capturing efficiency of the macro-device with FM-1 particles over a run time of 3 hours, corresponding to sixty-nine passes of the total volume.

Figure 4.9 Average capturing efficiency of the macro-device with FM-1 particles over a run time of 3 hours, corresponding to sixty-nine passes of the total volume.

The average capturing efficiency of the macro-device with FM-1 particles over a run time of 3 hours is shown in Figure 4.9. From this figure, it can be seen that the capturing process reached its maximal efficiency after 3 hours.

The initial concentration of FM-2 particles in diesel fuel oil for 30 minutes and 3 hours for the macro-device is shown in Figure 4.10. The cumulative number of FM-2 particles of all sizes per mL of diesel fuel oil at the beginning of the 30 minutes and 3 hours experiments was about 8000.
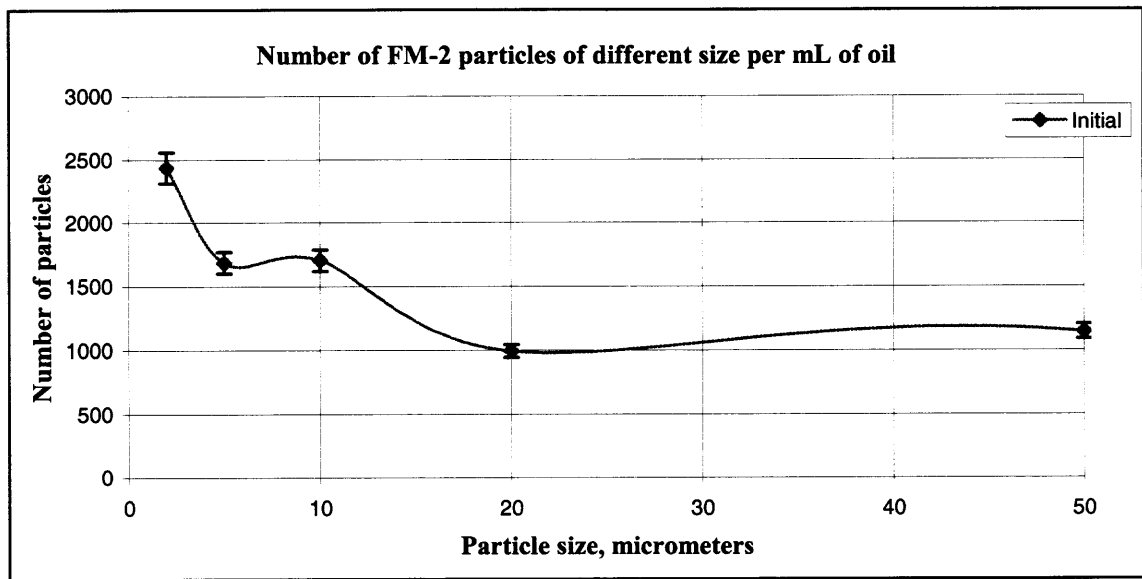
Figure 4.10 Initial number of FM-2 particles of different sizes per mL of diesel fuel oil.

The capturing efficiency of the macro-device with FM-2 particles over a run time of 30 minutes, corresponding to twelve passes of the total volume of the oil in the system, is shown in Figure 4.11. This figure demonstrates that the capturing process was not maximal during that time duration. The average capturing efficiency of the macro-device with FM-2 particles over a run time of 30 minutes is shown in Figure 4.12. The capturing efficiency was the largest for FM-2 particles of sizes ranging from 20 to 50 micrometers.

The capturing efficiency for FM-2 particles of sizes ranging from 50 to 75 micrometers was lower than that obtained for particles of smaller sizes because of the low concentration of these particles.
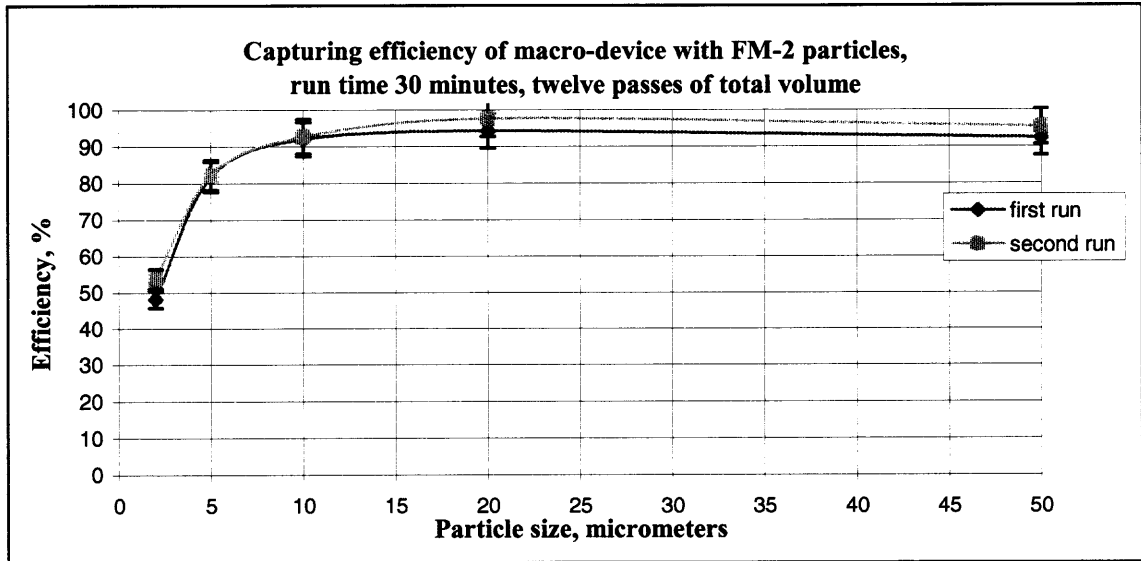

Figure 4.11 Capturing efficiency of the macro-device with FM-2 particles over a run time of 30 minutes, corresponding to twelve passes of the total volume.
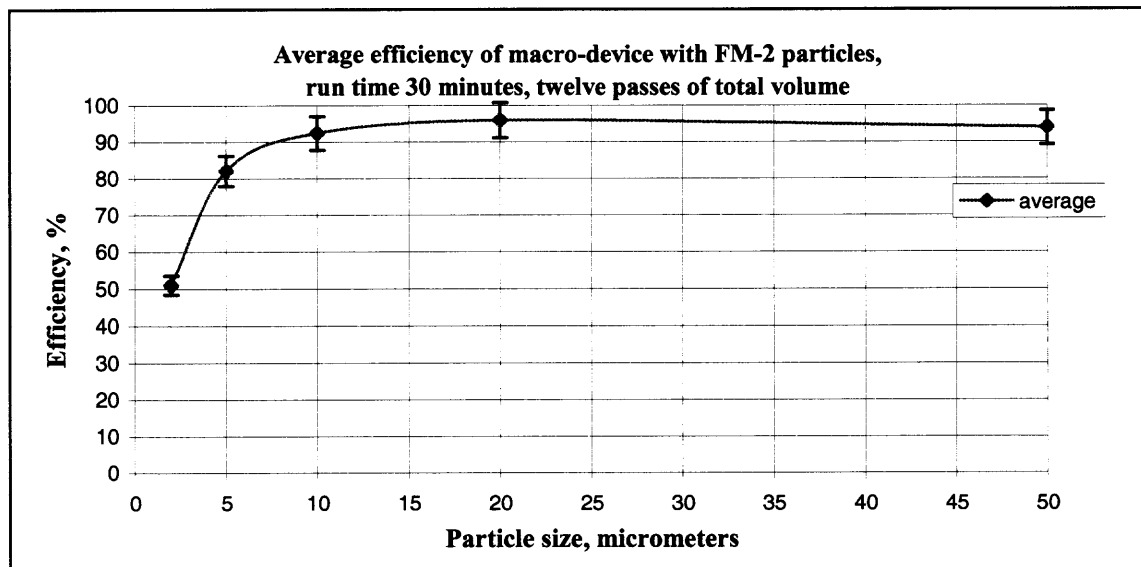

Figure 4.12 Average capturing efficiency of the macro-device with FM-2 particles over a run time of 30 minutes, corresponding to twelve passes of the total volume.

The capturing efficiency of the macro-device with FM-2 particles over a run time of 3 hours, corresponding to sixty-nine passes of the total volume of the oil in the system, is shown in Figure 4.13.
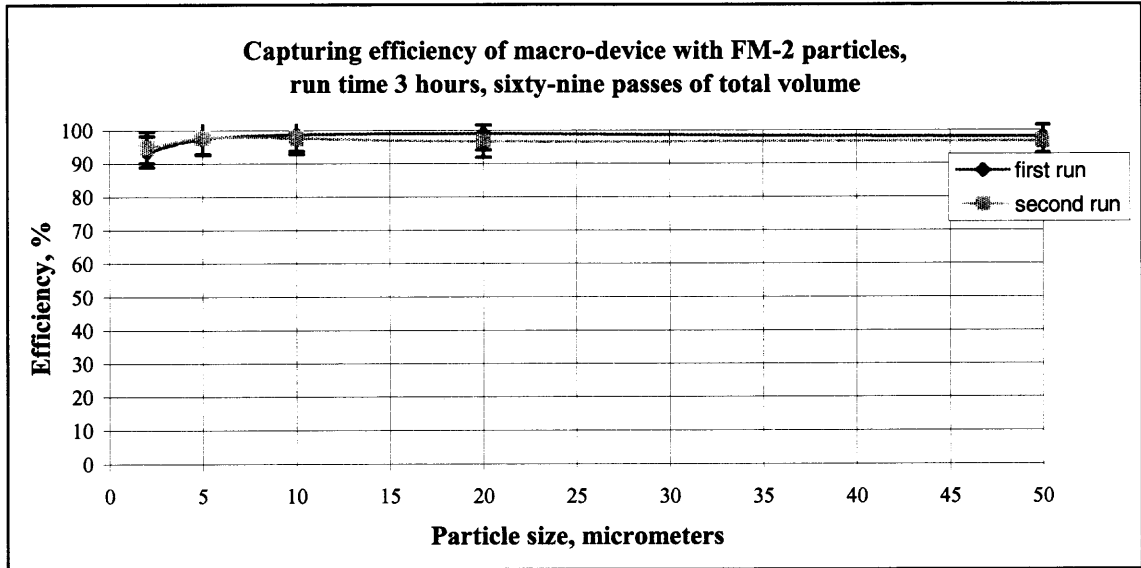

Figure 4.13 Capturing efficiency of the macro-device with FM-2 particles over a run time of 3 hours, corresponding to sixty-nine passes of the total volume.
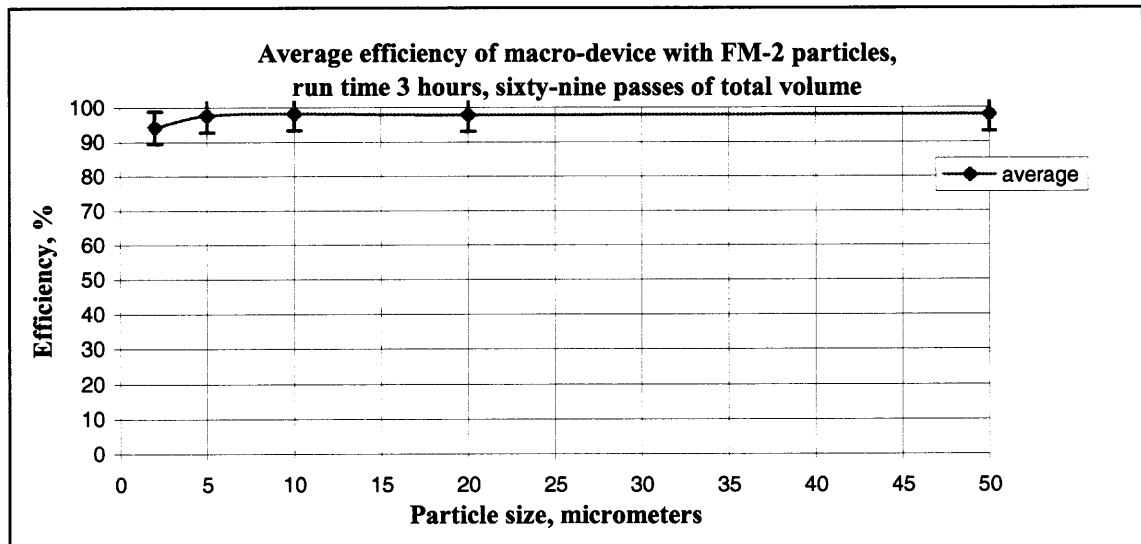

Figure 4.14 Average capturing efficiency of the macro-device with FM-2 particles over a run time of 3 hours, corresponding to sixty-nine passes of the total volume.

The average capturing efficiency of the macro-device with FM-1 particles over a run time of 3 hours is shown in Figure 4.14, demonstrating that the capturing process has reached its maximal capacity after 3 hours.

The comparison of the capturing efficiency of the macro-device for both FM-1 and FM-2 particles over a run times of 30 minutes and 3 hours is shown in Figure 4.15.
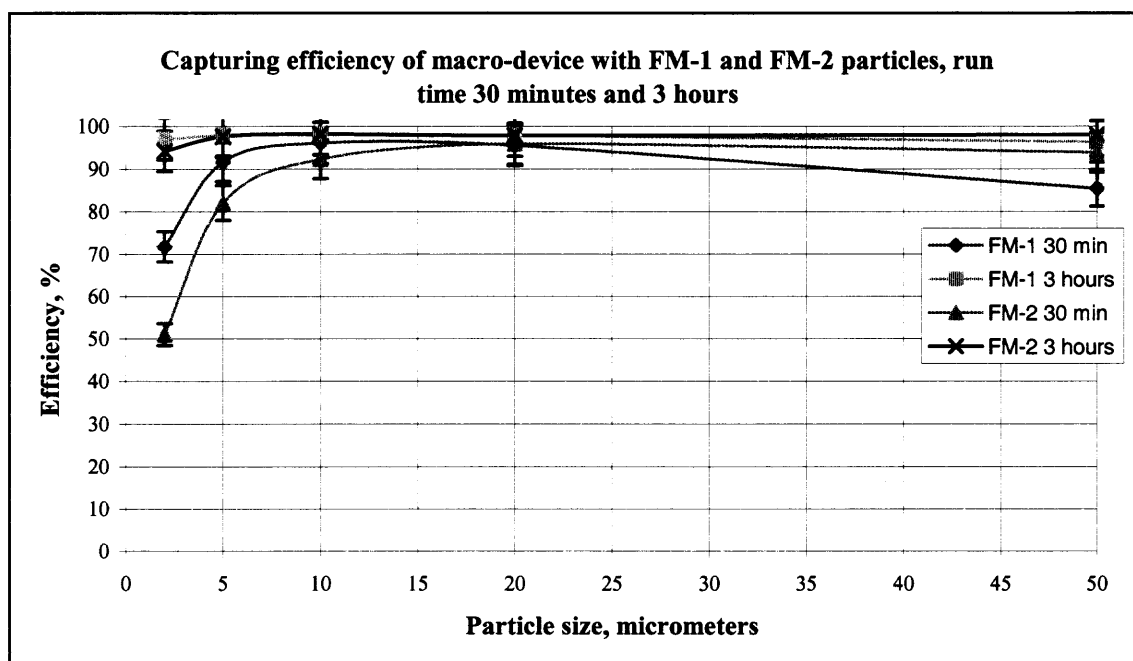

Figure 4.15 Comparison of the capturing efficiency of the macro-device for both FM-1 and FM-2 particles over a run times of 30 minutes and 3 hours.

The capturing efficiency of the macro-device for FM-1 and FM-2 particles was found to be better for FM-1 particles than for FM-2 particles. This result is somewhat in disagreement with Figure 4.4, which showed that the dielectrophoretic force had to be larger for FM-2 particles. A possible explanation for this disagreement is the possible influence of mutual dielectrophoresis, causing the pearl-chain formation inside the macro-device, and the influence of the fluid velocity, two phenomena ignored in Figure 4.4. The capturing efficiency for FM-1 and FM-2 particles of sizes ranging from 50 to 75

micrometers was lower than that obtained for particles of smaller sizes because of the low concentration of these particles. The concentration of the particles with sizes in the range of 50-75 micrometers was much lower than the concentration of other particles; therefore the error of the experimental results for the capturing efficiency of these particles was about 15%.

The initial concentration of FM-1 particles in diesel fuel oil for the 3 hour experiment using the micro-device is shown in Figure 4.16. The cumulative number of FM-1 particles of all sizes per mL of diesel fuel oil at the beginning of the experiment was about 7500.
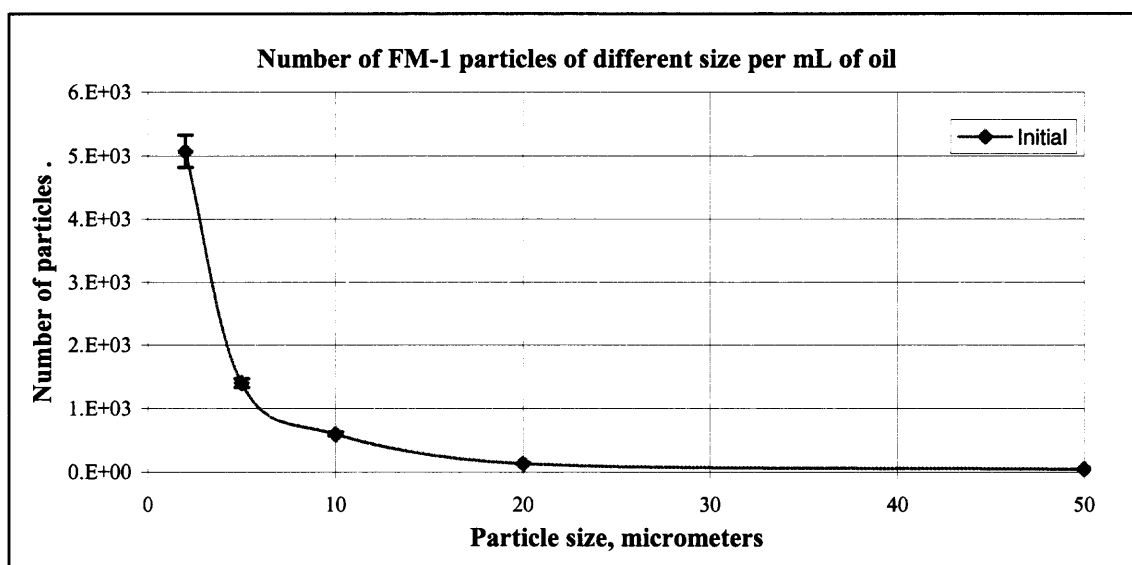

Figure 4.16 Initial number of FM-1 particles of different sizes per mL of diesel fuel oil.

The capturing efficiency of the micro-device with FM-1 particles over a run time of 3 hours, corresponding to two passes of the total volume of the oil in the system, is shown in Figure 4.17. This figure demonstrates that the capturing process was fully established and had the efficiency close to maximal after that time duration. The average

capturing efficiency of the micro-device with FM-1 particles over a run time of 3 hours is
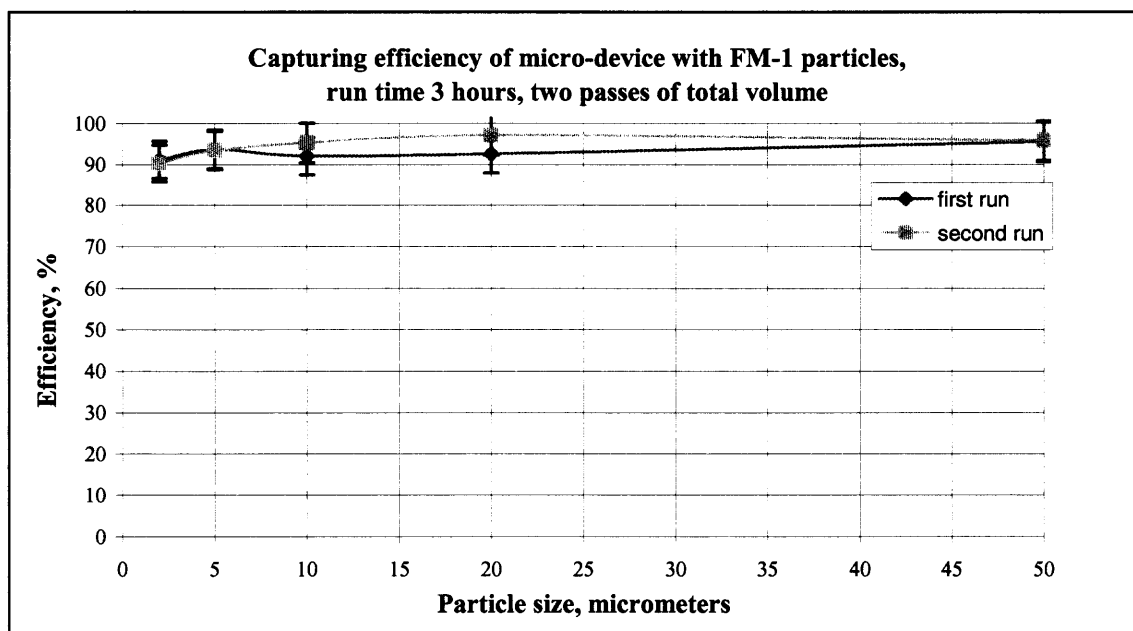
shown in Figure 4.18.

Figure 4.17 Capturing efficiency of the micro-device with FM-1 particles over a run time of 3 hours, corresponding to two passes of the total volume.
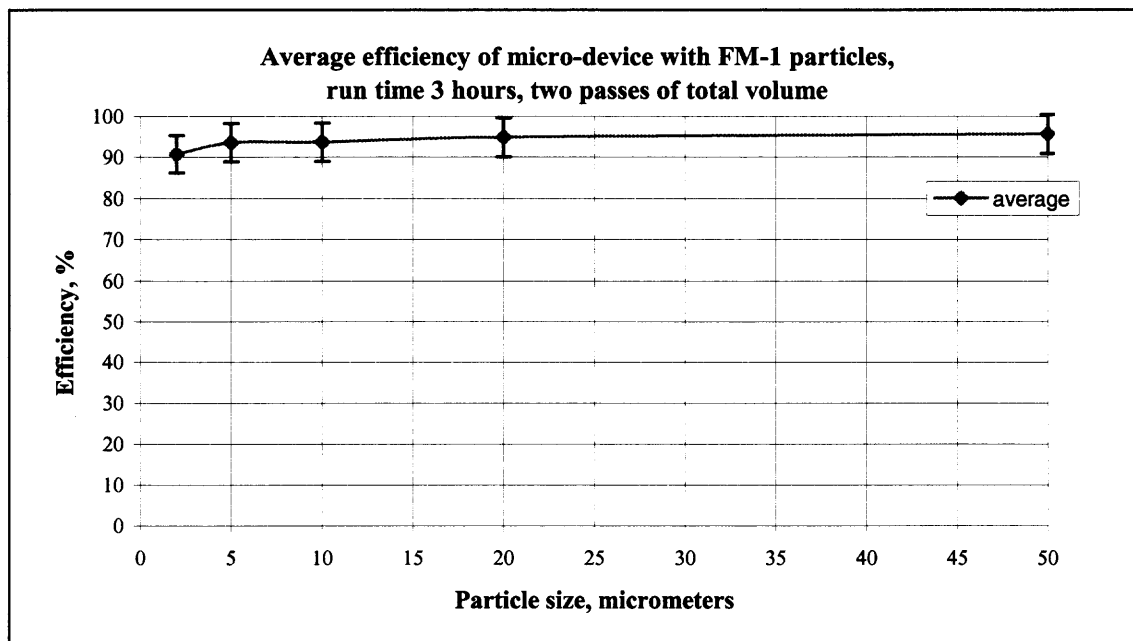

Figure 4.18 Average capturing efficiency of the micro-device with FM-1 particles over a run time of 3 hours, corresponding to two passes of the total volume.

The initial concentration of FM-2 particles in diesel fuel oil for the 3 hour experiments using the micro-device is shown in Figure 4.19. The cumulative number of FM-2 particles of all sizes per mL of diesel fuel oil at the beginning of the experiments was about 4000.
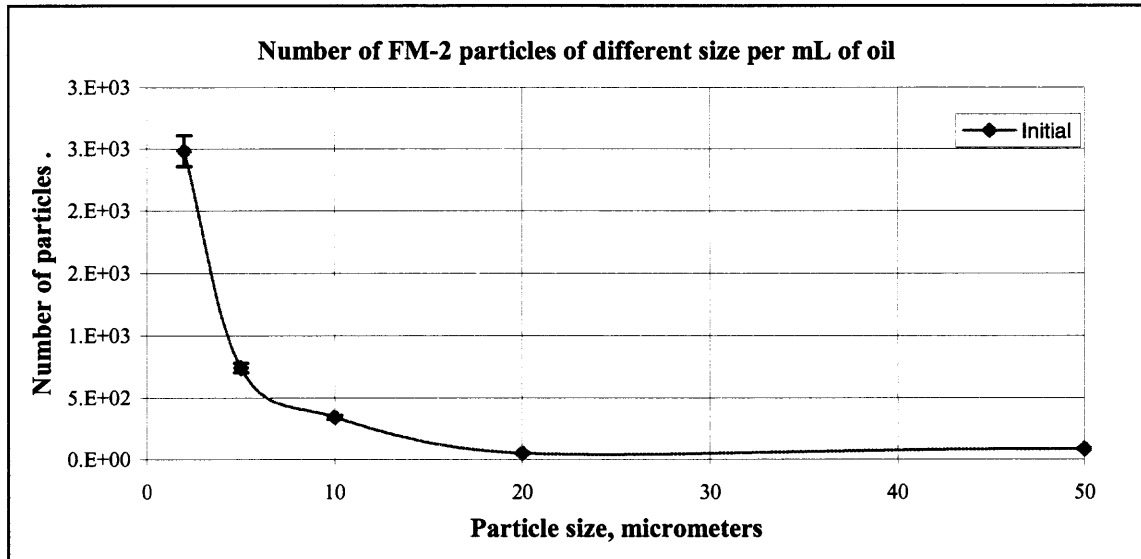

Figure 4.19 Initial number of FM-2 particles of different sizes per mL of diesel fuel oil.

The capturing efficiency of the micro-device with FM-2 particles over a run time of 3 hours, corresponding to two passes of the total volume of the oil in the system, is shown in Figure 4.20. This figure demonstrates that the capturing process of FM-2 particles had an efficiency close to maximal at that time. The average capturing efficiency of the micro-device with FM-2 particles over a run time of 3 hours is shown in Figure 4.21.
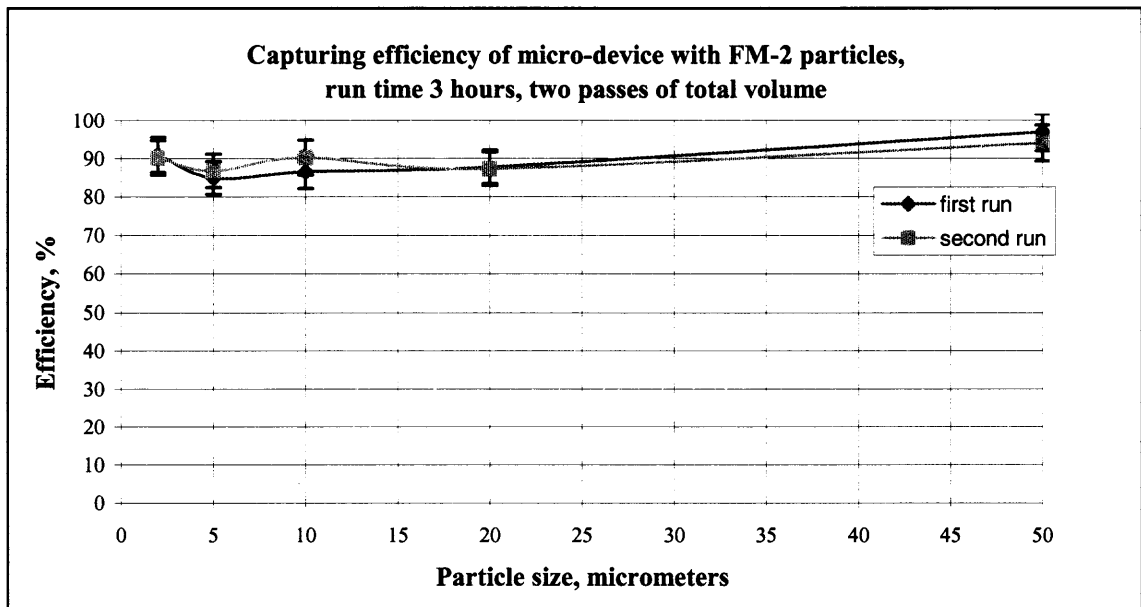
Figure 4.20 Capturing efficiency of the micro-device with FM-2 particles over a run time of 3 hours, corresponding to two passes of the total volume.
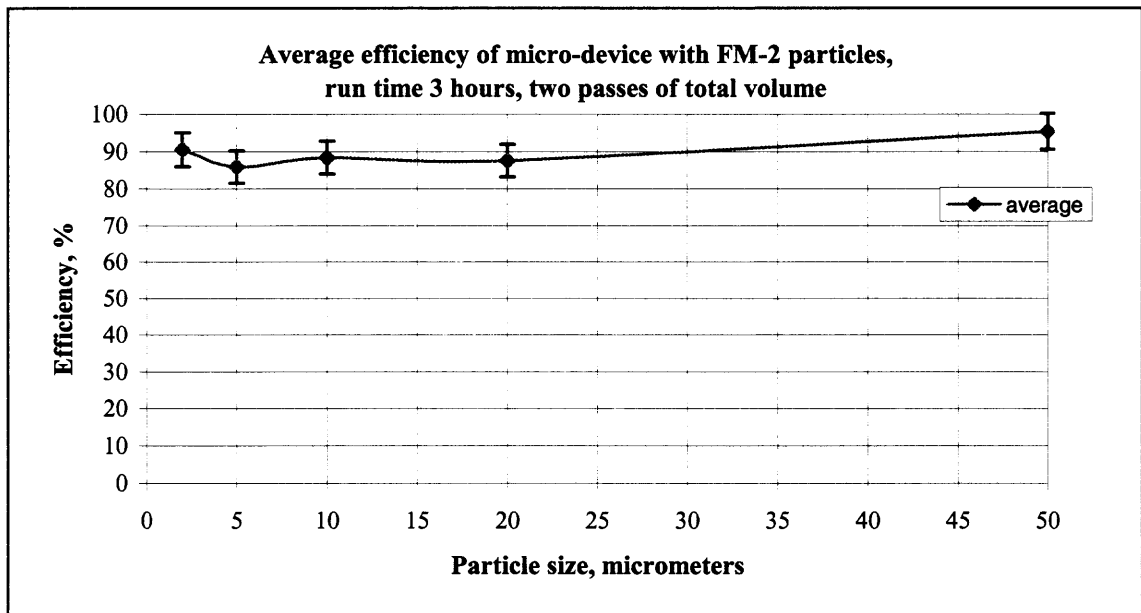

Figure 4.21 Average capturing efficiency of the micro-device with FM-2 particles over a run time of 3 hours, corresponding to two passes of the total volume.

The comparison of the capturing efficiency of the micro-device for FM-1 and FM-2 particles over a run time of 3 hours is shown in Figure 4.22.
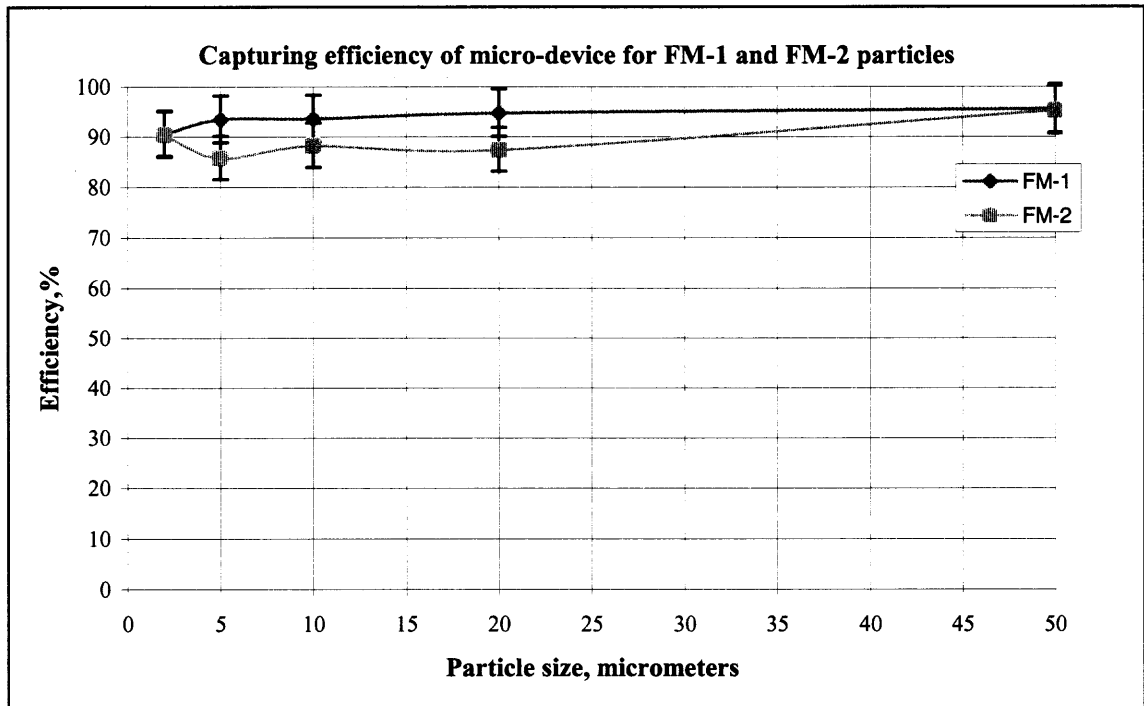

Figure 4.22 Comparison of the capturing efficiency of the micro-device for FM-1 and FM-2 particles over a run time of 3 hours.

It follows that the capturing efficiency of the micro-device for FM-1 and FM-2 particles demonstrates that the capturing efficiency was better for FM-1 particles than for FM-2 particles. This situation is similar to the case of the macro-device.

Figure 4.23 shows the comparison of the capturing efficiency between the macro- and micro-device after three hours. Recall that the number of passes of the total volume for the micro-device was equal to two and the number of passes of the total volume for the macro-device was equal to twelve.
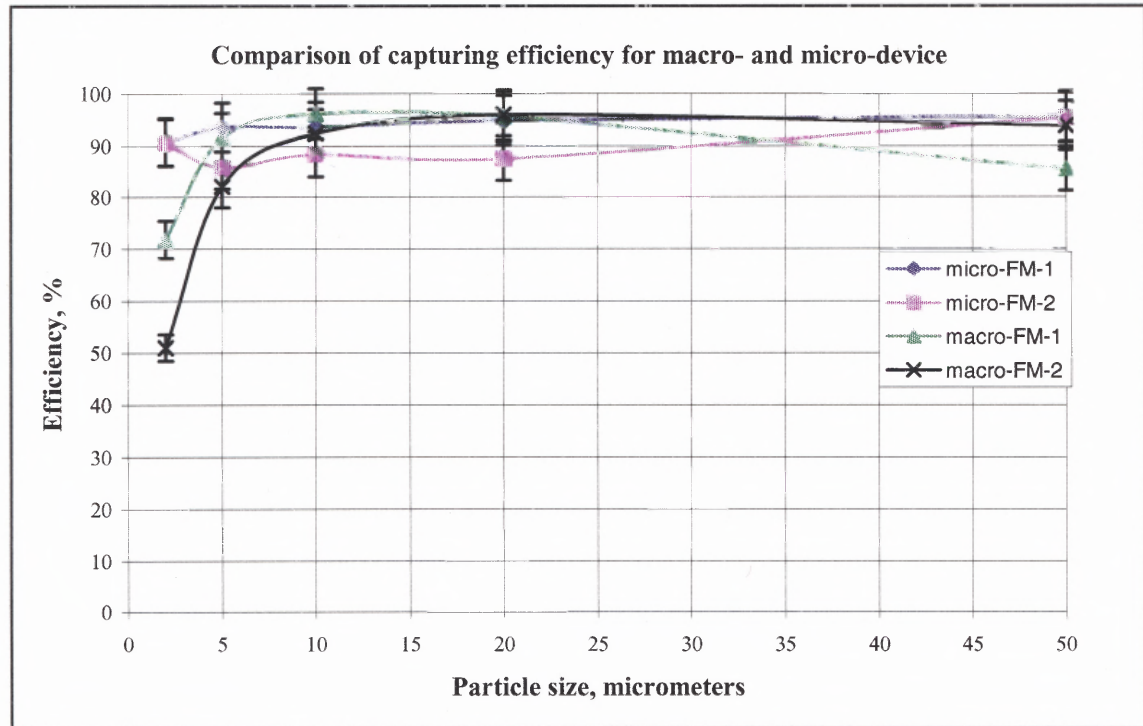
Figure 4.23 Comparison of capturing efficiency for macro- and micro-device with FM-1 and FM-2 particles.

Figure 4.23 demonstrates that the capturing efficiency for the micro-device was better than the capturing efficiency of the macro-device, even though the number of passes of the total volume in the micro-system was six times less than that in the macro-system. Particularly, a significant improvement of the capturing efficiency was found for particles of sizes in the range of 2-10 microns. This fact proves that the micro-device is a very efficient filtering device, which may even be used for particles sizes less than 2 micrometers. Therefore, miniaturization of the electrodes significantly increased the capturing efficiency of the experimental device.

4.4 Expression of Experimental Results in Differential Form

For many purposes, it is interesting to express results of this work in dimensionless form. The nondimensionalization of the equations of motion (2.10 – 2.12) shows that in addition to the Reynolds number, another parameter enters the equations:

$$P = \frac{2a^2\varepsilon_0 \, \mathrm{Re}\{f(\varepsilon_p,\varepsilon_m)\}V^2}{3\mu U h^3} \tag{4.8}$$

where ε_m and ε_p being the complex permittivities of the medium and the particle; $\varepsilon_0 = 8.854*10^{-12}$ C/Vm is the permittivity of free space; $\mathrm{Re}\{f(\varepsilon_p, \varepsilon_m)\}$ is taken from Formula (2.9); V is the voltage of the AC electric signal; $\mu_{oil}=2*10^{-2}$ (N*s/m^2) is the dynamic viscosity of diesel fuel oil; U is the velocity of the particles; and h is the distance between the electrodes.
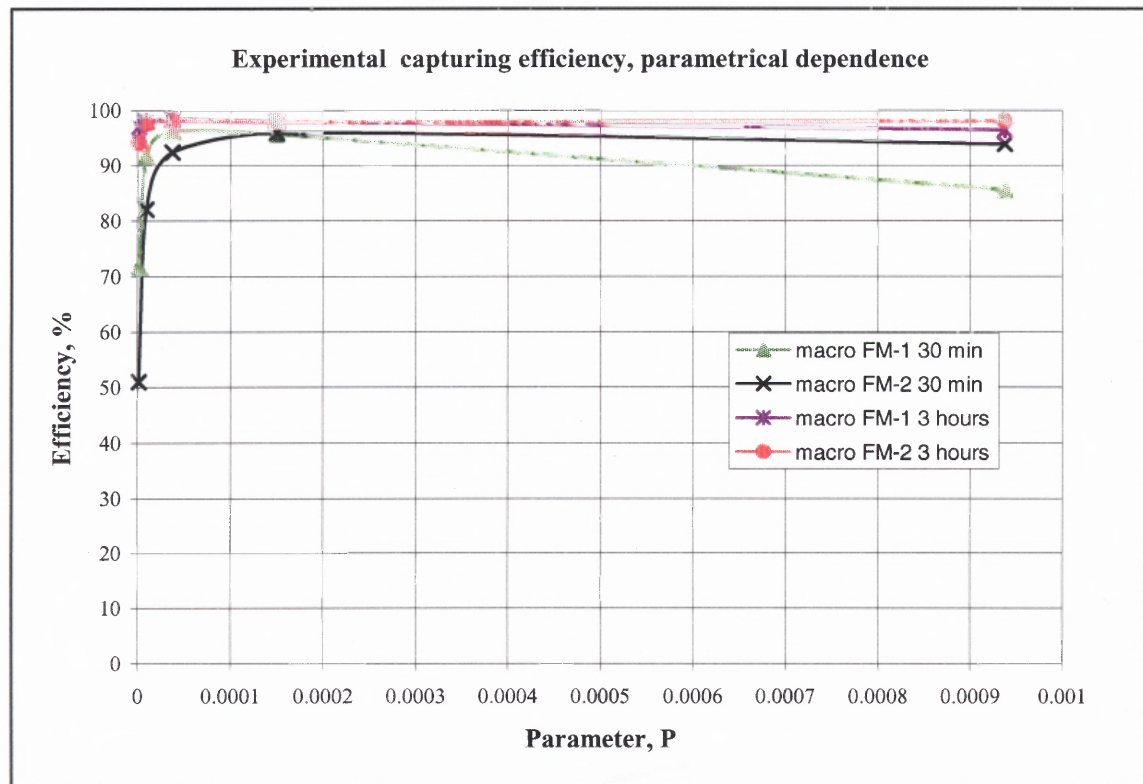

Figure 2.25 Parametrical dependence of the experimental capturing efficiency of the macro-device.

The experimental capturing efficiency in terms of non-dimensional parameter P is shown in Figure 2.25. In particular, this will allow direct comparison between experimental and numerical results.

CONCLUSIONS

This thesis has presented experimental results for the electrohydrodynamical manipulation of particles based on dielectrophoresis in two devices, a macro-device and a micro-device. The efficiency of particle capturing was determined experimentally for both devices. This study showed that the capturing efficiency of the micro-device is larger than the capturing efficiency of the macro-device for the same amount of time corresponding to a number of passes of the total volume of the oil in the micro-system six times less than that in the macro-system. It is thus concluded that miniaturization significantly increases the capturing efficiency of particles, in particular allowing the manipulation of very small size particles.

REFERENCES

Bottcher C.J.F., *Theory of electric polarization,* Elsevier Scientific Pub. Co., Amsterdam, New York, second edition, 1973-78.

Green N.G. and Morgan H., "Dielectrophoretic separation of nano-particles," *J. Phys. D, Applied Physics,* 30, L41-L84, 1997.

Hill N.E. and others, *Dielectric properties and molecular behavior,* Van Nostrand Reinhold, London, New York, 1969.

Hippel A., *Dielectric materials and applications,* Artech House, Boston, 1995.

Kawabata T., and Washizu M., "Dielectrophoretic detection of molecular bindings," *IEEE Trans. on Industry Applications,* vol. 37, No. 6, November/December 2001.

Loytsyanskiy L.G., *Mechanics of fluid and gas,* Nauka, Moscow, 5th edition, 1978.

Markx G.H. and Pethig R., "Dielectrophoretic separation of cells; continuous separation," *Biotechnol. Bioeng.,* 45, 337-343, 1995.

Pohl H.A., *Dielectrophoresis,* Cambridge University Press. 1978.

Shaw D.J., *Electrophoresis,* Academic P., London, New York, 1969.

Smyth C.P., *Dielectric behavior and structure; dielectric constant and loss, dipole moment and molecular structure,* McGraw-Hill, New York, 1955.

Solymar L. and Walsh D., *Electrical properties of materials,* Oxford University Press, Oxford, New York, 6th edition, 1998.

Suzuki S., Yamanashi T., Tazawa S., Kurosawa O., and Washizu M., "Quantitative analysis of DNA orientation in stationary AC electric fields using fluorescence anisotropy," *IEEE Trans. on Industry Applications,* vol. 34, No. 1, January/February 1998.

Tallan N.M., *Electrical conductivity in ceramics and glass,* Dekker M., New York, 1974.

Wang X.B., Huang Y., Burt J.P.H., Markx G.H., and Pethig R., "Dielectrophoretic confinement of bioparticles in potential energy wells," *J. Phys. D., Appl. Phys.,* 26, 1278-1285, 1993.